



# Optimization and characterization of new oleogels developed based on sesame oil and rice bran oil

Subajiny Sivakanthan<sup>a,b,c,1</sup>, Sabrina Fawzia<sup>d</sup>, Sagadevan Mundree<sup>e</sup>, Terrence Madhujith<sup>f</sup>, Azharul Karim<sup>a,\*</sup>

<sup>a</sup> School of Mechanical, Medical and Process Engineering, Faculty of Engineering, Queensland University of Technology, 2 George St, Brisbane City, QLD, 4000, Australia

<sup>b</sup> Department of Agricultural Chemistry, Faculty of Agriculture, University of Jaffna, Kilinochchi, 44000, Sri Lanka

<sup>c</sup> Postgraduate Institute of Agriculture, University of Peradeniya, Peradeniya, 20400, Sri Lanka

<sup>d</sup> School of Civil and Environmental Engineering, Faculty of Engineering, Queensland University of Technology, 2 George St, Brisbane City, QLD, 4000, Australia

<sup>e</sup> School of Biology and Environmental Science, Faculty of Science, Queensland University of Technology, 2 George St, Brisbane City, QLD, 4000, Australia

<sup>f</sup> Department of Food Science and Technology, Faculty of Agriculture, University of Peradeniya, Peradeniya, 20400, Sri Lanka

## ARTICLE INFO

### Keywords:

Beeswax  
Oleogel  
Optimization  
Rice bran oil  
Sesame oil  
Stearic acid

## ABSTRACT

In recent years, there has been a surge of interest in oleogels as a promising low-saturated and *trans* fat free alternative to traditional solid fats. However, to date, oleogels made from different edible oils using different gelator molecules have minimum commercial application due to the lack of mimicking the properties of conventional solid fats. This study aimed to optimize the formulation of oleogels with properties close to commercial margarines based on binary mixtures of sesame oil and rice bran oil using beeswax and stearic acid as oleogelators. An Extreme Vertices Design with four components: sesame oil, rice bran oil, beeswax, and stearic acid, and 32 runs was developed using Minitab 21.1. Multi-response optimization was performed based on rheological parameters, and oil binding capacity as responses. All responses for optimization had R<sup>2</sup> values > 96%. The oil binding capacity of the optimized oleogel was 99.99%. Optimized oleogel was further characterized for rheological, thermal, microstructural, and molecular properties and compared with commercial margarines. Results show that the properties of the optimized formula had closer values to those of commercial margarines, however with less structural recovery ability. Optimized oleogel exhibited higher oxidative stability than the margarine, however, lower than the oils. Beeswax and stearic acid exhibited synergistic effects on the oleogel properties at the ratio of 3:1. Results indicate that the optimized oleogel has the potential to be used in margarine manufacture with further developments to improve the gel strength and oxidative stability of the oleogel.

## 1. Introduction

Solid fat such as margarine is used as an ingredient in a variety of foods such as baked goods, confectioneries, and meat products to provide unique texture and flavor. Traditionally, margarines are manufactured using hardstock fats produced through an oil structuring approach called partial hydrogenation. Making solid fats through partial hydrogenation primarily on using high-melting crystalline triacylglycerols to form a crystal network. Since these triacylglycerols are rich in saturated fatty acids and *trans* fatty acids produced as by-products during partial hydrogenation, the resulting structured oil is unhealthy (Patel, 2015a).

Due to the strong association of increased risk of cardiovascular diseases and other non-communicable diseases with the consumption of saturated fatty acids and *trans* fatty acids, the World Health Organization (WHO) has recommended that the intake of saturated fats and *trans* fats should be less than 10% and 1% of total energy intake, respectively (WHO, 2018). As a result, scientists have explored ways to develop healthy solid fat alternatives. In this context, oleogelation has gained increased attention as the most promising oil structuring technique to manufacture solid-like lipids called oleogels that mimic the properties of traditional solid fats from highly unsaturated oils and without *trans* fatty acids. Oleogelation is the process of developing continuous gels in which

\* Corresponding author.

E-mail addresses: [subajiny.sivakanthan@hdr.qut.edu.au](mailto:subajiny.sivakanthan@hdr.qut.edu.au) (S. Sivakanthan), [sabrina.fawzia@qut.edu.au](mailto:sabrina.fawzia@qut.edu.au) (S. Fawzia), [sagadevan.mundree@qut.edu.au](mailto:sagadevan.mundree@qut.edu.au) (S. Mundree), [tmadhujith@agri.pdn.ac.lk](mailto:tmadhujith@agri.pdn.ac.lk) (T. Madhujith), [azharul.karim@qut.edu.au](mailto:azharul.karim@qut.edu.au) (A. Karim).

<sup>1</sup> Permanent address.

<https://doi.org/10.1016/j.foodhyd.2023.108839>

Received 17 February 2023; Received in revised form 11 April 2023; Accepted 28 April 2023

Available online 8 May 2023

0268-005X/© 2023 The Authors. Published by Elsevier Ltd. This is an open access article under the CC BY license (<http://creativecommons.org/licenses/by/4.0/>).

liquid oil is immobilized inside a three-dimensional network formed by gelator/s (oleogelator/structurant) (Wijarnprecha et al., 2019). Since oleogelation is a physical approach, it does not change the chemical nature of oils and does not produce any *trans* fatty acids.

Waxes are the most widely studied oleogelators owing to their gelling ability at low concentrations (Doan et al., 2015). Among different types of natural waxes, beeswax can form viscoelastic gels more easily (Han et al., 2022; Oh et al., 2017). The major disadvantage of the use of wax as an oleogelator is the waxy mouth feel provided by wax. Therefore, combining wax with another oleogelator could contribute to reducing the amount of wax needed to make gel. Furthermore, many researchers have reported the synergistic effect among oleogelators when used together at specific proportions and concentrations (Sintang et al., 2017; Yang et al., 2020). In this study, stearic acid has been selected based on preliminary experiments to be used with beeswax. Stearic acid is also reported to possess gelling characteristics as well as beneficial health effects (Hunter et al., 2010; Sagiri et al., 2015). This study focused on developing an oleogel from two functional edible oils; sesame oil and rice bran oil, that contain high amount of polyunsaturated fatty acids and bioactive compounds with anti-inflammatory and antioxidant properties, which contribute to reduce the risk of cardiovascular diseases (Jayaraj et al., 2020; Liang et al., 2014; Punia et al., 2021). Even though different types of oils have been used to develop oleogels, sesame oil and rice bran oil got only a little attention from researchers.

The structure and properties of oleogels are affected by various factors including the structure and composition of oil and oleogelator, amount of oleogelator, processing parameters, and the interactions among different factors (Co & Marangoni, 2012; Patel, 2017; Thakur et al., 2022). Therefore, it is crucial to find suitable combinations of oil and oleogelators and processing conditions in order to develop oleogel with desired properties. This study primarily considered the optimum mixture of oils and oleogelators and the oleogels are produced under the processing conditions which are determined by the preliminary experiments.

The interactions between the oleogelator/s, and the oil/s have a major influence on oleogel properties (Barroso et al., 2020). The physicochemical properties of the oils such as degree of unsaturation, chain length, viscosity, and polarity are also related to the formation of gel network structure (Han et al., 2022). For example, the polarity of oil and the presence of functional moieties with hydrogen bonding sites and long alkyl chains in the oleogelator molecule influence the interactions between oil and oleogelator resulting in modifications in the gel structure (Patel, 2018). There is a large body of evidence on the literature regarding the use of various oleogelator and oil combinations to develop oleogels. Nevertheless, the attempts to modulate the properties of oleogels by changing the oil composition and other properties via blending of different oils are much limited. A few studies have been reported on using oil blends for making oleogels (Sagiri et al., 2015), however, they did not consider systematically evaluating different combinations of oils. The present study is designed to select the optimum mixture of selected oleogelators and oils to develop oleogel with properties close to commercial margarines.

Optimization is essential in food engineering to develop a product with desired characteristics (Palla et al., 2017). Mixture design is a type of Response Surface Methodology (RSM) used in the optimization of components in a mixture and process parameters. The advantage of this method compared to the full factorial designs is that this optimization technique provides a large volume of information from a relatively small number of experiments. A few recent studies have focused on optimizing different oleogel systems using RSM and the optimized oleogels have been compared with commercial margarines and shortenings (Alizadeh et al., 2020; Ghan et al., 2022; Naeli et al., 2022; Palla et al., 2017; Thakur et al., 2022). To the best of the author's knowledge, no studies have been carried out for the optimization of oleogel or the development of oleogel based on sesame oil, rice bran oil, beeswax, and stearic acid.

This study aimed at developing oleogel intended to be used in margarine manufacture. Margarine is an oil-in-water emulsion containing not less than 80% fat. The structure and properties of margarine is primarily influenced by the fat portion and the properties of the gel network (Abdolmaleki et al., 2022). Therefore, it is important to develop oleogels that bear properties similar to margarines. Therefore, this study used commercial margarines as the reference. This study hypothesized that synergistic interaction between beeswax and stearic acid and changing oil composition and properties by blending sesame oil and rice bran oil could enhance and result in the properties of oleogel close to the commercial margarines. Therefore, the optimum combination of sesame oil, rice bran oil, beeswax, and stearic acid that can produce the oleogel with maximum oil binding capacity and mechanical properties close to the commercial margarines was determined by a mathematical optimization technique, Mixture Design using Minitab 21.1. Optimization was performed using rheological properties as well as oil binding capacity as the responses to optimize the mixture of oils and oleogelators. Optimized oleogel was further characterized by the physical, mechanical, microstructural, molecular, and thermal properties and compared with the commercial margarines.

## 2. Materials and methods

### 2.1. Materials

Oil samples such as sesame oil (Changs, Thailand), and rice bran oil (Alfa one, USA) were purchased from a local grocery store in Brisbane, Australia. Fatty acid compositions of the oils were analyzed by GC (Shimadzu, Japan). Sesame oil contained  $0.24 \pm 0.03\%$  of C14:0,  $9.8 \pm 0.03\%$  of C16:0,  $37.29 \pm 0.83\%$  of C18:1, and  $52.66 \pm 1.21\%$  of C18:2. Rice bran oil contained  $22.54 \pm 0.40\%$  of C16:0,  $43.41 \pm 0.19\%$  of C18:1 and  $33.46 \pm 0.85\%$  of C18:2. Beeswax (refined) (melting point as determined by differential scanning calorimetry was  $62.2 \pm 0.56$  °C) and stearic acid (melting point as determined by differential scanning calorimetry was  $56.30 \pm 0.14$  °C, and the fatty acid composition as determined by GC was C12:0 - <1%, C14:0 - <2%, C16:0 - 43%, and C18:0 - 54%), chemicals, reagents, and standards were purchased from Sigma Aldrich, Australia. Four different brands of commercial margarines were purchased from local grocery store in Brisbane, Australia.

### 2.2. Design of experiment

In order to determine the optimum mixture composition of the oleogel, Extreme Vertices Design with 32 runs was created using Minitab 21.1 (Minitab, LLC, USA) with the design degree of 3 (Table 1). The mixture components used were the amount of two oleogelators and two oils. The design was created to keep the mixture total of 1. All runs were performed in triplicates. The upper and lower values of the components used in the design of experiments were determined during the preliminary experiments. Gel formation of oleogelators was evaluated at 5%, 10%, and 15% (w/w). Minimum oleogelator concentrations were 5% (w/w) for beeswax and 10% for stearic acid as single oleogelator based on the tilt test (formation of self-standing gels upon inversion of tubes). The lower and upper values of beeswax and stearic acid were chosen as 0–0.15 and 0–0.10, respectively (for the mixture total of 1), because it was decided to evaluate the effect of single oleogelator and the mixtures of oleogelators to determine any potential synergistic interactions among the oleogelators. Since the minimum oleogelator concentration of beeswax was lower than that of stearic acid, the maximum amount of beeswax was kept higher than that of stearic acid to reduce the total amount of oleogelators in the final optimized formulation. The amount of oleogelator ranged from 5 to 25% of the total mixture on weight basis. Since both sesame oil and rice bran oil were able to form gels with the selected oleogelators and considering their nutritional significance, the upper and lower values of both oils were kept the same. Since both oils have good nutritional and

**Table 1**

Design of experiments and responses for oleogels prepared from rice bran oil and sesame oil using beeswax and stearic acid.

Run Order	Mixture composition				Responses					
	SO (g)	RBO (g)	BW (g)	SA (g)	OBC (%)	Gel point (°C)	G' at LVR (Pa)	Flow $\tau$ (Pa)	Flow $\gamma$	Flow G' (Pa)
1	0.5000	0.2500	0.1500	0.1000	98.56 ± 1.41	63.51 ± 0.41	6.18E+05 ± 2.25E+04	1,212.50 ± 71.42	4.03 ± 0.54	2.16E+04 ± 1.34E+03
2	0.3000	0.5000	0.1500	0.0500	99.51 ± 0.60	64.32 ± 0.69	2.68E+05 ± 6.72E+02	657.20 ± 66.19	14.16 ± 0.30	2.96E+03 ± 6.36E+01
3	0.4250	0.4250	0.1500	0.0000	97.42 ± 1.14	67.27 ± 1.03	1.14E+05 ± 8.53E+03	337.35 ± 30.48	32.27 ± 0.75	2.16E+03 ± 1.46E+02
4	0.4125	0.4125	0.0750	0.1000	88.41 ± 4.63	58.60 ± 0.96	1.07E+05 ± 2.51E+04	172.10 ± 94.89	31.04 ± 3.95	5.06E+02 ± 7.85E+00
5	0.2500	0.5000	0.1500	0.1000	98.73 ± 1.77	63.15 ± 0.52	4.06E+05 ± 3.09E+04	735.75 ± 120.99	25.71 ± 1.59	1.13E+04 ± 1.98E+02
6	0.5000	0.3250	0.0750	0.1000	88.90 ± 3.21	57.50 ± 1.44	8.71E+04 ± 7.77E+03	164.05 ± 48.01	34.13 ± 8.17	4.05E+02 ± 7.21E+00
7	0.3393	0.4643	0.1179	0.0786	98.61 ± 0.5	62.08 ± 0.12	2.29E+05 ± 2.70E+04	499.25 ± 25.95	20.91 ± 2.73	2.33E+03 ± 1.53E+02
8	0.5000	0.5000	0.0000	0.0000	–	–	–	–	–	–
9	0.4500	0.4500	0.0000	0.1000	95.37 ± 0.26	51.48 ± 2.22	1.94E+04 ± 5.55E+03	31.38 ± 1.41	39.76 ± 2.13	5.49E+01 ± 1.53E+00
10	0.4643	0.3393	0.1179	0.0786	98.88 ± 0.50	61.82 ± 0.41	3.15E+05 ± 3.24E+04	920.75 ± 6.01	21.53 ± 4.08	3.07E+03 ± 1.38E+02
11	0.5000	0.3000	0.1500	0.0500	98.61 ± 0.74	64.03 ± 0.35	3.19E+05 ± 4.00E+04	992.15 ± 13.93	9.12 ± 1.72	4.58E+03 ± 5.04E+02
12	0.4667	0.4667	0.0000	0.0667	54.31 ± 4.30	48.03 ± 2.52	2.20E+04 ± 2.47E+03	32.04 ± 1.65	39.74 ± 2.38	5.73E+01 ± 6.31E+00
13	0.4643	0.4643	0.0429	0.0286	40.15 ± 3.50	54.82 ± 3.16	2.93E+02 ± 8.11E+00	0.76 ± 0.11	1.28 ± 0.13	4.21E+01 ± 2.83E-02
14	0.5000	0.3750	0.0750	0.0500	93.87 ± 2.87	58.03 ± 1.79	6.02E+04 ± 2.75E+04	19.18 ± 5.32	8.43 ± 3.67	1.45E+02 ± 7.04E+00
15	0.4500	0.4500	0.1000	0.0000	97.12 ± 0.07	63.78 ± 0.33	7.47E+04 ± 9.11E+03	63.81 ± 17.61	13.69 ± 3.22	3.61E+02 ± 2.19E+00
16	0.5000	0.4250	0.0750	0.0000	88.03 ± 0.36	60.11 ± 1.26	1.94E+04 ± 4.33E+03	9.44 ± 1.01	3.15 ± 0.56	2.74E+02 ± 1.91E+01
17	0.5000	0.3500	0.1500	0.0000	99.41 ± 0.76	66.16 ± 1.06	3.75E+05 ± 2.51E+04	1,038.65 ± 178.69	28.42 ± 3.03	3.77E+03 ± 1.87E+02
18	0.4143	0.4643	0.0429	0.0786	59.24 ± 3.41	54.21 ± 3.09	3.78E+04 ± 9.95E+03	36.52 ± 8.41	12.14 ± 2.92	3.14E+02 ± 1.14E+01
19	0.4643	0.4143	0.0429	0.0786	63.31 ± 4.32	56.02 ± 1.42	4.21E+04 ± 6.59E+03	39.35 ± 1.63	11.91 ± 1.97	2.72E+02 ± 2.07E+01
20	0.4286	0.4286	0.0857	0.0571	97.54 ± 0.96	59.28 ± 1.08	1.05E+05 ± 3.53E+03	118.80 ± 5.66	23.74 ± 4.57	3.98E+02 ± 4.17E+00
21	0.4643	0.3893	0.1179	0.0286	98.73 ± 0.50	62.95 ± 0.41	2.13E+05 ± 9.60E+03	515.65 ± 17.47	26.92 ± 2.21	1.36E+03 ± 1.56E+01
22	0.3893	0.4643	0.1179	0.0286	98.92 ± 1.22	63.80 ± 0.93	1.63E+05 ± 2.21E+04	244.95 ± 25.67	21.08 ± 4.91	1.16E+03 ± 7.14E+01
23	0.4000	0.5000	0.0000	0.1000	92.83 ± 1.98	51.97 ± 1.71	2.13E+04 ± 6.35E+02	34.72 ± 4.99	46.07 ± 8.21	5.54E+01 ± 1.70E+01
24	0.5000	0.4000	0.0000	0.1000	93.72 ± 2.72	47.70 ± 3.33	1.87E+04 ± 1.56E+03	27.55 ± 7.69	36.39 ± 4.60	7.57E+01 ± 7.48E+00
25	0.3750	0.3750	0.1500	0.1000	99.07 ± 1.22	62.46 ± 1.17	4.35E+05 ± 3.33E+04	1,604.00 ± 12.73	19.27 ± 0.98	5.89E+03 ± 2.50E+02
26	0.5000	0.4500	0.0000	0.0500	13.01 ± 0.63	37.47 ± 2.27	1.74E+02 ± 3.34E+01	1.53 ± 1.61	3.59 ± 0.13	8.55E+00 ± 1.50E+00
27	0.4000	0.4000	0.1500	0.0500	98.93 ± 0.84	63.32 ± 1.87	2.77E+05 ± 2.24E+04	770.10 ± 37.05	27.61 ± 2.31	1.99E+03 ± 1.18E+02
28	0.4250	0.5000	0.0750	0.0000	90.45 ± 3.82	57.68 ± 1.20	2.07E+04 ± 1.96E+03	19.18 ± 3.65	4.85 ± 0.92	2.76E+02 ± 6.51E+00
29	0.4500	0.5000	0.0000	0.0500	17.84 ± 1.63	39.88 ± 0.56	2.71E+02 ± 2.78E+01	0.80 ± 0.22	10.91 ± 1.30	5.12E+00 ± 8.44E-01
30	0.3500	0.5000	0.1500	0.0000	99.70 ± 0.43	66.02 ± 2.28	3.22E+05 ± 2.23E+04	697.10 ± 110.87	26.85 ± 6.12	3.37E+03 ± 9.55E+01
31	0.3250	0.5000	0.0750	0.1000	87.95 ± 3.59	57.57 ± 0.53	6.21E+04 ± 1.48E+03	78.97 ± 11.41	22.07 ± 1.75	2.67E+02 ± 1.66E+01
32	0.3750	0.5000	0.0750	0.0500	92.18 ± 3.43	56.76 ± 0.77	6.77E+04 ± 1.62E+03	85.71 ± 8.17	26.77 ± 1.20	2.43E+02 ± 1.82E+01
	Commercial margarine 1				70.13 ± 0.45	56.29 ± 0.80	4.93E+04 ± 2.01E+03	255.10 ± 37.10	14.90 ± 1.03	1.21E+03 ± 1.25E+02
	Commercial margarine 2				79.65 ± 0.03	55.77 ± 0.94	7.16E+04 ± 5.94E+03	302.33 ± 33.29	12.44 ± 2.06	1.74E+03 ± 1.96E+02
	Commercial margarine 3				78.65 ± 0.26	57.83 ± 0.83	7.26E+04 ± 8.27E+03	338.05 ± 16.33	12.74 ± 0.22	1.89E+03 ± 1.23E+02
	Commercial margarine 4				78.38 ± 0.69	61.02 ± 0.73	7.86E+04 ± 8.80E+03	372.50 ± 37.48	11.73 ± 0.08	2.26E+03 ± 2.08E+02

BW: beeswax, LVR: linear viscoelastic range, OBC: oil binding capacity, RBO: rice bran oil, SA: stearic acid, SO: sesame oil.

therapeutic values, it is decided to use both oils in the final formulation. Therefore, the lower values of the oils were not chosen to be 0 to create the design of experiments.

### 2.3. Analysis of the design of experiments and multi-response optimization

The responses used for the optimization were oil binding capacity and rheological properties such as storage modulus ( $G'$ ) at Linear Viscoelastic Range (LVR), flow tau ( $\tau$ ), flow gamma ( $\gamma$ ), flow  $G'$  and gel point. The same parameters of 4 different brands of commercial solid fat samples (margarines) were also determined. Optimization was performed by setting the value for oil binding capacity as the maximum (100%) and the values for rheological parameters close to the commercial margarines. The robustness of the design was analyzed using regression for mixtures. The statistical significance of the quadratic model factors and the robustness of the models were determined using Analysis of Variance (ANOVA) with  $p$  values  $< 0.05$  considered significant. Regression equations for the responses were created by backward elimination of terms. The correlation between different responses was analyzed using Pearson correlation method. The optimization was performed based on the highest value of oil binding capacity (100%) and the target values of other responses to produce oleogel samples with rheological properties closer to commercial margarines. The optimum formulation selected from the design was analyzed further for rheological, thermal, and molecular properties and microstructure.

### 2.4. Preparation of oleogels

Oleogels were prepared by direct dispersion of oleogelators in the oil. Oil and oleogelators were weighed into the tubes as per the experimental design shown in Table 1. The contents in the tubes were heated at 85 °C under constant stirring (200 rpm) for 30 min using an orbital shaking water bath (Stuart SBS40, China). The liquid mixtures were then cooled and stored at 20 °C for 48 h before analysis. All measurements were performed at 20 °C. Preliminary experiments were carried out to find out the effective process parameters. Two different heating temperatures (65 and 85 °C) and shaking speeds (100 rpm and 200 rpm) were evaluated by determining the hardness of the oleogel using a texture analyzer (IMADA FRTS 100 N, Japan) (data not provided). The heating temperature of 85 °C and shaking speed of 200 rpm were found to produce the gel with high hardness values. Therefore, these conditions were used to make oleogels for optimization studies.

### 2.5. Analysis of oleogel

#### 2.5.1. Oil binding capacity

The oil binding capacity of the oleogels was determined as explained by Guo et al. (2020) with slight modifications. The sample was heated to melt completely, and 1 mL of the hot liquid mixture was transferred into a previously weighed (W1) 2 mL centrifuge tube. The liquid sample in the tube was allowed to set under the same conditions of oleogelation and incubated at  $20 \pm 1$  °C for 48 h. The tube with gel was weighed again (W2) and centrifuged at 13000 rpm for 15 min at 20 °C in a centrifuge (Ependorf, MiniSpin, Germany). Then, the tubes were inverted for 1 h to drain the liquid oil, and the tubes after draining were weighed (W3). Oil binding capacity was calculated using the following equation.

$$\text{Oil binding capacity (\%)} = 1 - \frac{W2 - W3}{W2 - W1} \times 100 \quad (1)$$

#### 2.5.2. Rheology

The rheological properties of the oleogels were analyzed using a Rheometer (Anton Paar MCR302 Rheometer, Austria) with the TruSt-rain™ option, analysis software: RheoCompass™ version 1.30.999. and

a Peltier temperature control unit using sand-blasted parallel plate geometry (diameter of 50 mm, PP50-S). A normal force of 0.1 N was applied to make sure that the plate has a good grip on the sample. All experiments were carried out at 20 °C after 48 h of storage.

**2.5.2.1. Amplitude sweep and frequency sweep.** Amplitude sweep and frequency sweep tests were performed according to the method explained by Aguilar-Zárate et al. (2019) with some modifications. An amplitude sweep was performed with strain values ranging from 0.01 to 100% with a frequency of 1 Hz to find out the LVR. The LVR was observed from the amplitude sweeps as a plateau for the  $G'$  and  $G''$ . The following parameters were determined from amplitude sweep: LVR limit,  $G'$  at LVR, loss factor, flow  $\tau$ , flow  $\gamma$ , and flow  $G'$ . Frequency sweeps (0.01–100 Hz) were then performed at a strain value within LVR. These experiments were conducted at an initial fixed gap of 0.5 mm.

**2.5.2.2. Temperature ramp test.** The dynamic temperature ramp test was carried out from 20 to 70 °C at the rate of 2 °C min<sup>-1</sup> at a frequency of 1 Hz and a strain value within LVR. These experiments were conducted at an initial fixed gap of 1.0 mm. The gel point/crossover temperature was determined as the crossover point of  $G'$  and  $G''$  ( $G' = G''$ ).

**2.5.2.3. Thixotropy.** To evaluate the structural recovery ability (thixotropy), oleogels were subjected to a 3ITT, Rot-Rot-Rot (3 interval) thixotropy test. Samples were subjected to alternative cycles of low and high shear rates (0.1 s<sup>-1</sup> for the first 10 min (interval 1) followed by 10 s<sup>-1</sup> for 5 min (interval 2) and 0.1 s<sup>-1</sup> for the last 10 min (interval 3)) (Patel & Dewettinck, 2015). The structure recovery was calculated by considering the viscosity value at the end of interval 1 as 100% and comparing it with the peak viscosity value in interval 3 (Tavernier et al., 2018). These experiments were conducted at an initial fixed gap of 0.5 mm.

#### 2.5.3. Thermal analysis

Thermal parameters such as the onset of crystallization, onset of melting, peak melting and peak crystallization, and enthalpies of melting and crystallization of neat oleogelators and oleogels were determined using Differential Scanning Calorimetry (DSC) (DSC 204 F1 Phoenix, Netzsch, Germany) as explained by Doan et al. (2017) with some modifications. The oleogel samples were subjected to heating and cooling cycles under a nitrogen atmosphere. The thermal program consisted of heating at 85 °C for 10 min to remove all the crystalline history before cooling to 0 °C at the rate of 2 °C/min, keeping isothermally at 0 °C for 20 min, and reheating to 85 °C at the rate of 5 °C/min. Melted samples ( $10 \pm 1$  mg) were placed in sealed aluminium crucibles. An empty crucible was used as the reference. The data were analyzed using Netzsch Proteus® software.

#### 2.5.4. Oxidation behavior

Thermogravimetric analysis (TGA) curves were obtained for dynamic (non-isothermal) heating experiment using Simultaneous Thermal Analyzer (Jupiter STA 449 F3, Netzsch, Germany). For the dynamic heating experiments, samples ( $5 \pm 0.4$  mg) were added into 80  $\mu$ L platinum pans without lids and heated from 30 to 700 °C at a heating rate of 20 °C per min under air (20% oxygen and 80% nitrogen) at a flow rate of 50 mL min<sup>-1</sup>. Oxidation induction time and oxidation induction temperature were determined as the intercept point by tangent method (extrapolated onset) using Netzsch Proteus® software.

#### 2.5.5. Fourier transform infrared (FTIR) spectroscopy

The FTIR spectra of the samples were obtained within the range of 4000 and 400 cm<sup>-1</sup> using a Fourier transform infrared spectrometer (Nicolet iS50 FT-IR, Thermo Scientific, USA) with a resolution of 4 cm<sup>-1</sup>. A total of 64 scans were collected at room temperature and the peaks were analyzed to identify the interactions between beeswax and stearic

acid.

### 2.5.6. Polarized light microscopy

Microstructure of the oleogels was observed using Nikon Eclipse LV100ND (Nikon Instruments Inc., USA) polarized light microscopy provided with a digital camera (Nikon DS-Fi2). A drop of the melted oleogel was placed on a preheated glass slide and a cover slip was put on and stored for 48 h at 20 °C before imaging. Images were acquired at 20 °C at a magnification of 200 × and images were processed with Nikon NIS Elements software.

### 2.6. Statistical analysis

Statistical analyses were performed using the Minitab 21.1 software package (Minitab, LLC, USA). Values are expressed as mean ± standard deviation. One-way ANOVA and Duncan's test were employed to measure the statistical significance. The significance level used was 95% ( $p < 0.05$ ).

## 3. Results and discussion

The best oleogelator for a particular oil type to make oleogel with desired properties cannot be easily predicted because the structure of an oleogel is a result of complex interactions between the characteristics of the oleogelator and oil (Fayaz et al., 2020). Therefore, it is necessary to find suitable oleogelator/s for the particular oil type/s. Preliminary studies were carried out to select suitable oleogelators. For this purpose, experiments were carried out using beeswax, stearic acid, and lauric acid as the oleogelators at the concentrations of 5, 10, and 15% (w/w), and based on the visual observation of tilt test, beeswax, and stearic acid were selected to make oleogels from rice bran oil and sesame oil and their combinations. Lauric acid did not form gel either alone or in combination with the other two oleogelators. Based on the visual observation by the tilt test, 5% (w/w) of beeswax and 10% (w/w) of stearic acid formed self-standing gels in sesame oil. Martins et al. (2016) and Li et al. (2022) also reported that beeswax was able to form self-sustaining gels at a concentration of 4% and above. Patel et al. (2015) reported the critical gelling concentration of beeswax for the gelation of high oleic sunflower oil as 1% (w/w) which was determined by rheological characterization (frequency sweep). Sagiri et al. (2015) reported that the critical oleogelator concentrations determined by the tilt test for stearic acid to make oleogel using sesame oil and soybean oil were 16% (w/w) and 19% (w/w), respectively. The differences in the minimum or critical gelling concentrations for the same oleogelator reported in the literature could be due to the technique used.

Further, exploration of synergistic effects among oleogelators for particular oil types could enhance the properties of the oleogels. Since, making oleogels using all possible combinations of oleogelators and oils to find the best combinations is practically impossible or time consuming, in this study, it has been decided to evaluate the selected oleogelators alone as well as in combinations systematically using a statistical approach to select the best performing oleogelators or oleogelator mixtures and their concentration for the selected oil mixture.

This study considered oil binding capacity and rheological properties as responses for optimization. Oil binding capacity is the amount of oil entrapped in the network structure after providing centrifugal force (Flöter et al., 2021). It gives information on the ability of the 3D gel network to entrap the oil (Thakur et al., 2022). Since oleogels are prepared to contain a high proportion of oil (>90%), oleogels should have high oil binding capacity to avoid oil leakage.

Oleogel is a viscoelastic material, that is, it exhibits both viscous and elastic characteristics. From a rheological point of view, oleogels are characterized by elastic portion,  $G'$ , which demonstrates a distinct plateau and by a loss modulus (viscous portion),  $G''$ , lesser than the  $G'$  in the plateau region (Okuro et al., 2021). Determination of  $G'$  and  $G''$  with regard to frequency, stress/strain time, and temperature are important

for the characterization of oleogel. Amplitude sweep, frequency sweep, and temperature ramp experiments are the most common rheological tests performed to characterize oleogels. Amplitude sweep and frequency sweep experiments give details about the microstructural strength of the oleogels (Tavernier et al., 2018). Amplitude rheograms can be viewed into two regions: LVR, where  $G'$  and  $G''$  remain constant with increasing strain and the deformation of the structure is reversible and non-linear visco-elastic region, where  $G'$  and  $G''$  start to decline with an increasing strain. With further increase in the strain,  $G'$  and  $G''$  crossover occurs, and the point is called the crossover point/flow point (Naeli et al., 2022). A temperature ramp test was carried out to determine the gel point temperature and an amplitude sweep test to find  $G'$  at LVR, flow  $\tau$ , flow  $\gamma$ , and  $G'$  at flow point (flow  $G'$ ). Measuring these rheological properties can provide valuable information on the properties of oleogels to select the oleogel formulation with desirable properties. Therefore, this study has chosen oil binding capacity and rheological properties as the responses for the optimization of oleogel mixture to produce an oleogel with properties close to that of commercial solid fats. The  $G'$  values of all oleogels prepared according to the design were greater than their corresponding  $G''$  within the LVR, confirming that all samples exhibited solid-like behavior.

### 3.1. Analysis of experimental design

The properties (responses) of oleogels prepared according to the mixture design are shown in Table 1 and a summary of ANOVA for the regression analysis of the design is shown in Table 2. Regression analysis was performed to evaluate the significant effects ( $p < 0.05$ ) of linear, cubic, and quadratic terms. The coefficient of determinations such as  $R^2$ ,  $R^2(\text{adj})$  (a measure of the amount of variation around the mean explained by the model), and  $R^2(\text{pred})$  (a measure of the amount of variation in new data explained by the model) are used to explain how well the model fits the data (Palla et al., 2017). ANOVA tables showed that all responses were significantly affected by the oils and oleogelators with  $R^2$  higher than 96% indicating the robustness of the model for the optimization. Previous studies also reported that the  $R^2$  value above 90% is adequate for optimization of oleogelation (Palla et al., 2017; Thakur et al., 2022). Ghan et al. (2022) reported  $p$  values of above 89% for the responses for the optimization of mixture for soy lecithin and glyceryl monostearate based oleogel using Extreme Vertices Design. Further, in this study,  $R^2(\text{adj})$  and  $R^2(\text{pred})$  were also higher than 93% for all responses indicating the robust fit of the models to the responses except for  $R^2(\text{pred})$  for flow  $\gamma$ , which was 87.09%. However, the difference between  $R^2(\text{pred})$  and  $R^2(\text{adj})$  less than 20% is acceptable to explain the model (Palla et al., 2017). Therefore, the data for the flow  $\gamma$  were also well-fitted to the model. The Lack of Fit is another important measure that explains whether the model accurately fits the data. If the  $p$  value is significant ( $p < 0.05$ ), the model does not fit the data. In this study, all responses except for flow  $\gamma$  showed significant  $p$  values ( $p > 0.05$ ). Therefore, it can be concluded that the data fit the models very well for the optimization study except for the flow  $\gamma$ .

#### 3.1.1. Model fitting

The model fitting was performed by the backward elimination of terms, a kind of stepwise regression that removes the terms that are not significant (with  $p$  values higher than 0.05). Table 3 illustrates the ANOVA for the fitted models for the responses used in optimization of the design. Both linear as well as interaction terms were included in model fitting. Both oils had significant linear effect on the oil binding capacity, gel point,  $G'$  at LVR and flow  $\tau$ , whereas the oleogelators beeswax and stearic acid did not exhibit significant linear effect on the responses. The interaction effects of oils and oleogelators on all responses were significant ( $p < 0.05$ ). Regression equations have been developed for each response by Fit Regression Model and they are discussed below to describe the relationship between the response and the terms in the model. Coefficient of determinations such as  $R^2$ ,  $R^2(\text{adj})$ ,

**Table 2**

Regression coefficients and probabilities for the responses.

Source	Gel point	OBC	G' at LVR	Flow $\tau$	Flow $\gamma$	Flow G'
Regression	<0.0001	<0.0001	<0.0001	<0.0001	<0.0001	<0.0001
Linear	0.001	<0.0001	0.086	0.010	<0.0001	<0.0001
Quadratic	<0.0001	<0.0001	<0.0001	<0.0001	<0.0001	<0.0001
Full Cubic	<0.0001	<0.0001	0.002	0.001	<0.0001	<0.0001
Special Quartic	<0.0001	<0.0001	<0.0001	<0.0001	<0.0001	<0.0001
Full Quartic1	<0.0001	<0.0001	<0.0001	<0.0001	<0.0001	<0.0001
Lack-of-Fit	0.487	0.598	0.073	0.135	0.007	0.054
R <sup>2</sup> (%)	99.44	98.60	99.43	99.31	96.98	99.82
R <sup>2</sup> (adj) (%)	98.86	97.16	98.84	98.60	93.87	99.63
R <sup>2</sup> (pred) (%)	97.59	94.02	97.56	97.04	87.09	99.23

OBC: oil binding capacity.

and R<sup>2</sup>(pred) are used to explain how well the models for each response fits the data.

Pearson correlation analysis was performed to understand the relationship between different responses. According to the correlation analysis, flow  $\tau$  and flow  $\gamma$ , flow  $\gamma$  and G' at LVR, and flow  $\gamma$  and flow G' combinations showed negative nonsignificant ( $p > 0.05$ ) correlations, whereas all other combinations of the responses had positive significant ( $p < 0.02$ ) correlations, except for the combination of gel point and flow  $\gamma$  ( $p = 0.83$ ).

**3.1.1.1. Oil binding capacity.** As presented in Table 1, the oil binding capacities of the majority of the oleogel formulations (26 samples out of 32 samples) were not significantly different among them with the values ranging from 87.95 to 99.70%. The lowest values for oil binding capacity (13.01–17.84%, w/w) were shown by the oleogels prepared only using stearic acid at the concentration of 5% (w/w) (runs 26 and 29). The samples of the runs 12 and 13, which were prepared using 7.14% and 7.69% of oleogelator, also had very low oil binding capacity (54.3% and 40.15%, respectively). Similar values for the oil binding capacity have been reported by other researchers as well. Thakur et al. (2022) reported the oil binding capacity of the oleogels developed from soybean oil using carnauba wax (5–15%) for the optimization study as 68.76–99.73%. Oil binding capacity ranging from 16 to 98.7% was reported for the optimization of oleogel based on binary and ternary mixtures of sodium caseinate (0–4%), xanthan gum (0–1%) and guar gum (0–1%) (Abdolmaleki et al., 2020).

Regression analysis of the model showed that oil binding capacity was significantly influenced by the interactions among the oils and oleogelators. This is evident from the highly significant  $p$  values for the interaction effects among oils, and oleogelators and between the oils and oleogelators as shown in Table 1. The best model created by backward elimination of terms describing the relationship between oil binding capacity and the factors is given in equation (2) ( $R^2 = 93.86\%$ ). The R<sup>2</sup>(adj) and R<sup>2</sup>(pred) were in good agreement (92.94% and 91.96%, respectively). In this model, all the terms are highly significant ( $p < 0.0001$ ) except for SO  $\times$  RBO ( $p = 0.043$ ) and SO  $\times$  RBO  $\times$  SA ( $p = 0.034$ ) which had significant  $p$  value and SO  $\times$  RBO  $\times$  BW ( $p = 0.097$ ) which had non-significant effect. Similarly, R<sup>2</sup> values of above 90% were reported for the model created for oil binding capacity by Palla et al. (2017) for the optimization of processing parameters to develop oleogels from high oleic sunflower oil and Myverol and Thakur et al. (2022) for the optimization of processing conditions and oleogelator concentration.

$$\text{Oil binding capacity} = -1882 + 1775 \text{ SO} + 1733 \text{ RBO} + 619 \text{ SO} \times \text{RBO} + 3097 \text{ SO} \times \text{BW} + 2991 \text{ SO} \times \text{SA} + 3373 \text{ RBO} \times \text{BW} + 3613 \text{ RBO} \times \text{SA} + 15695 \text{ BW} \times \text{SA} - 2383 \text{ SO} \times \text{RBO} \times \text{BW} - 3368 \text{ SO} \times \text{RBO} \times \text{SA} - 16250 \text{ SO} \times \text{BW} \times \text{SA} - 20474 \text{ RBO} \times \text{BW} \times \text{SA} \quad (2)$$

**3.1.1.2. Gel point.** Temperature ramp experiments were performed to

examine the effect of temperature on the gelling characteristics of the oleogel and to determine the crossover temperature/gel point/gel-sol transition temperature ( $G'' = G'$ ). The gel point of the samples ranged from  $37.47 \pm 2.27$  °C to  $66.16 \pm 1.06$  °C. Samples with a high proportion of beeswax as oleogelator showed high gel points, whereas samples with less proportion of beeswax or stearic acid as the only oleogelator exhibited lower gel point values. As determined by the DSC, the melting point of the beeswax was  $62.2 \pm 0.56$  °C and the stearic acid was  $56.30 \pm 0.14$  °C. Therefore, it could be interpreted that the type and amount of oleogelators determined the gel point of the samples. According to the correlation analysis, gel point showed a strong positive correlation with G' at LVR and oil binding capacity ( $p < 0.0001$ ). The best model created by backward elimination of terms describing the relationship between the gel point and the factors is given in equation (3) ( $R^2 = 93.86\%$ ). The R<sup>2</sup>(adj) and R<sup>2</sup>(pred) were 92.94% and 91.96% respectively, which were in accordance with each other.

$$\text{Gel point} = -1882 + 1775 \text{ SO} + 1733 \text{ RBO} + 619 \text{ SO} \times \text{RBO} + 3097 \text{ SO} \times \text{BW} + 2991 \text{ SO} \times \text{SA} + 3373 \text{ RBO} \times \text{BW} + 3613 \text{ RBO} \times \text{SA} + 15695 \text{ BW} \times \text{SA} - 2383 \text{ SO} \times \text{RBO} \times \text{BW} - 3368 \text{ SO} \times \text{RBO} \times \text{SA} - 16250 \text{ SO} \times \text{BW} \times \text{SA} - 20474 \text{ RBO} \times \text{BW} \times \text{SA} \quad (3)$$

All the terms are highly significant ( $p < 0.0001$ ) in this model except for SO  $\times$  RBO ( $p = 0.043$ ) and SO  $\times$  RBO  $\times$  SA ( $p = 0.034$ ) and SO  $\times$  RBO  $\times$  BW ( $p = 0.097$ ).

**3.1.1.3. G' at LVR.** The LVR in an amplitude sweep rheogram indicates the range of G' in which the experiment can be performed without any damage to the structure of the sample. The values of G' in the LVR can give information on the viscoelastic character (structural strength) of the sample. As shown in Table 1, the G' at LVR ranged from  $1.74\text{E}+02 \pm 3.34\text{E}+01$  to  $6.18\text{E}+05 \pm 2.25\text{E}+04$ . The samples of runs 13, 26, and 29 had very low G' values which were prepared with a total oleogelator concentration of 5.26–7.69% (w/w). These values are in agreement with the oil binding capacities of the same samples as they had very low oil binding capacities because G' at LVR determines the structural strength of the oleogel. This relationship can be further confirmed by the strong positive correlation ( $p < 0.0001$ ) between these two parameters as shown by the results of correlation analysis. Moreover, G' at LVR showed strong positive correlation with other responses such as gel point, flow  $\tau$ , and flow G' ( $p < 0.0001$ ). Therefore, G' at LVR should be considered as an important quality parameter of the oleogels.

The best model created by backward elimination of terms describing the relationship between G' at LVR and the factors is given in equation (4) ( $R^2 = 94.72\%$ ). The R<sup>2</sup>(adj) and R<sup>2</sup>(pred) were in good agreement (93.45% and 91.14% respectively).

$$\text{G' at LVR} = -9.112\text{E}+7 + 8.027\text{E}+7 \text{ SO} + 8.044\text{E}+7 \text{ RBO} + 4.243 \text{E}+7 \text{ SO} \times \text{RBO} + 2.154\text{E}+8 \text{ SO} \times \text{BW} + 1.902\text{E}+8 \text{ SO} \times \text{SA} + 2.132\text{E}+8 \text{ RBO} \times \text{BW} + 1.905\text{E}+8 \text{ RBO} \times \text{SA} + 1.138\text{E}+9 \text{ BW} \times \text{SA} - 4.424\text{E}+8 \text{ SO} \times \text{RBO} \times \text{BW} - 3.392\text{E}+8 \text{ SO} \times \text{RBO} \times \text{SA} - 2.108\text{E}+8 \text{ SO} \times \text{BW} \times \text{SA} - 2.148\text{E}+9 \text{ RBO} \times \text{BW} \times \text{SA} + 3.775\text{E}+9 \text{ SO} \times \text{RBO} \times \text{BW} \times \text{SA} \quad (4)$$

**Table 3**  
ANOVA for the fitted models for the responses used in optimization design.

Source	DF	Adj SS	Adj MS	F-Value	P-Value
<b>Oil binding capacity</b>					
Regression	12	4459.65	371.637	101.93	<0.0001
SO	1	114.89	114.893	31.51	<0.0001
RBO	1	109.58	109.582	30.06	<0.0001
SO × RBO	1	15.39	15.394	4.22	0.043
SO × BW	1	60.56	60.561	16.61	<0.0001
SO × SA	1	63.31	63.312	17.37	<0.0001
RBO × BW	1	71.84	71.844	19.71	<0.0001
RBO × SA	1	92.42	92.425	25.35	<0.0001
BW × SA	1	91.33	91.331	25.05	<0.0001
SO × RBO × BW	1	10.29	10.291	2.82	0.097
SO × RBO × SA	1	16.91	16.914	4.64	0.034
SO × BW × SA	1	69.21	69.208	18.98	<0.0001
RBO × BW × SA	1	109.86	109.861	30.13	<0.0001
Error	80	291.68	3.646		
Total	92	4751.32			
<b>Gel point</b>					
Regression	12	4459.65	371.637	101.93	<0.0001
SO	1	114.89	114.893	31.51	<0.0001
RBO	1	109.58	109.582	30.06	<0.0001
SO × RBO	1	15.39	15.394	4.22	0.043
SO × BW	1	60.56	60.561	16.61	<0.0001
SO × SA	1	63.31	63.312	17.37	<0.0001
RBO × BW	1	71.84	71.844	19.71	<0.0001
RBO × SA	1	92.42	92.425	25.35	<0.0001
BW × SA	1	91.33	91.331	25.05	<0.0001
SO × RBO × BW	1	10.29	10.291	2.82	0.097
SO × RBO × SA	1	16.91	16.914	4.64	0.034
SO × BW × SA	1	69.21	69.208	18.98	<0.0001
RBO × BW × SA	1	109.86	109.861	30.13	<0.0001
Error	80	291.68	3.646		
Total	92	4751.32			
<b>G' at LVR</b>					
Regression	13	1.5898E+12	1.2229E+11	74.52	<0.0001
SO	1	2.3618E+10	2.3618E+10	14.39	<0.0001
RBO	1	2.3727E+10	2.3727E+10	14.46	<0.0001
SO × RBO	1	1.0293E+10	1.0293E+10	6.27	0.015
SO × BW	1	2.1194E+10	2.1194E+10	12.91	0.001
SO × SA	1	1.5469E+10	1.5469E+10	9.43	0.003
RBO × BW	1	2.0749E+10	2.0749E+10	12.64	0.001
RBO × SA	1	1.5506E+10	1.5506E+10	9.45	0.003
BW × SA	1	3.4405E+10	3.4405E+10	20.96	<0.0001
SO × RBO × BW	1	1.9861E+10	1.9861E+10	12.1	0.001
SO × RBO × SA	1	9816457081	9816457081	5.98	0.018
SO × BW × SA	1	2.6819E+10	2.6819E+10	16.34	<0.0001
RBO × BW × SA	1	2.7807E+10	2.7807E+10	16.94	<0.0001
SO × RBO × BW × SA	1	1.8595E+10	1.8595E+10	11.33	0.001
Error	54	8.8624E+10	1641180467		
Total	67	1.6785E+12			
<b>Flow τ</b>					
Regression	12	11582767	965231	132.55	<0.0001
SO	1	87038	87038	11.95	0.001
RBO	1	92886	92886	12.76	0.001
SO × BW	1	237156	237156	32.57	<0.0001
SO × SA	1	105046	105046	14.43	<0.0001
RBO × BW	1	170768	170768	23.45	<0.0001
RBO × SA	1	76139	76139	10.46	0.002
BW × SA	1	438416	438416	60.21	<0.0001
SO × RBO × BW	1	434967	434967	59.73	<0.0001
SO × RBO × SA	1	38431	38431	5.28	0.026
SO × BW × SA	1	501976	501976	68.93	<0.0001
RBO × BW × SA	1	469940	469940	64.53	<0.0001
SO × RBO × BW × SA	1	446962	446962	61.38	<0.0001
Error	53	385945	7282		
Total	65	11968712			
<b>Flow γ</b>					
Regression	4	7806.3	1951.58	37.08	<0.0001
SO × RBO × BW	1	4401.9	4401.91	83.63	<0.0001
SO × RBO × SA	1	7037.8	7037.77	133.7	<0.0001
RBO × BW × SA	1	372.6	372.57	7.08	0.010

**Table 3 (continued)**

Source	DF	Adj SS	Adj MS	F-Value	P-Value
SO × RBO × BW × SA	1	2612.3	2612.31	49.63	<0.0001
Error	67	3526.7	52.64		
Total	71	11333			
<b>Flow G'</b>					
Regression	9	1082204694	120244966	127.84	<0.0001
BW	1	16032127	16032127	17.04	<0.0001
SO × BW	1	15875162	15875162	16.88	<0.0001
SO × SA	1	20482700	20482700	21.78	<0.0001
RBO × BW	1	18761236	18761236	19.95	<0.0001
RBO × SA	1	14758910	14758910	15.69	<0.0001
SO × RBO × SA	1	18545808	18545808	19.72	<0.0001
SO × BW × SA	1	91658563	91658563	97.45	<0.0001
RBO × BW × SA	1	54371015	54371015	57.8	<0.0001
SO × RBO × BW × SA	1	84583222	84583222	89.92	<0.0001
Error	55	51733140	940603		
Total	64	1133937834			

BW: beeswax, LVR: linear viscoelastic range, OBC: oil binding capacity, RBO: rice bran oil, SA: stearic acid, SO: sesame oil.

All the terms are highly significant ( $P < 0.0001$ ) in this model except for  $SO \times BW$  ( $p = 0.001$ ),  $RBO \times BW$  ( $p = 0.001$ ),  $SO \times RBO \times BW$  ( $p = 0.001$ ),  $SO \times RBO \times BW \times SA$  ( $p = 0.001$ ),  $RBO \times SA$  ( $p = 0.003$ ),  $SO \times RBO \times SA$  ( $p = 0.018$ ) and  $SO \times RBO$  ( $p = 0.015$ ).

**3.1.1.4. Flow  $\tau$  (flow stress), flow  $\gamma$  (flow strain) and flow  $G'$ .** This study also determined the flow  $\tau$  (shear stress at flow point), flow  $\gamma$  (shear strain at flow point), and  $G'$  at flow point from the amplitude sweep rheogram. At the flow point where  $G' = G''$ , the gel structure of the material is deformed, and transformed into liquid state (viscous behaviour dominates the elastic behaviour). Samples with higher flow  $\gamma$  will have a high structural stability against deformation with increasing strain. As already discussed, flow  $\tau$  and flow  $\gamma$  ( $p = 0.74$ ), flow  $\gamma$  and flow  $G'$  ( $p = 0.14$ ) showed weak negative correlations, whereas flow  $\tau$  and flow  $G'$  had a strong positive correlation ( $p < 0.0001$ ). Moreover, these flow point parameters had significant correlations with other responses, however the correlation were weak. The weak correlations of flow properties with other responses can be understood from the results presented in Table 1. Flow  $\tau$ , flow  $\gamma$ , and  $G'$  at the flow point of the samples ranged from  $0.76 \pm 0.11$  to  $1,604 \pm 12.73$  Pa,  $1.28 \pm 0.13$  to  $46.07 \pm 8.21$  and  $5.12 \pm 0.84$  to  $2.16 \times 10^4 \pm 1.34 \times 10^3$  Pa, respectively.

The best model created by backward elimination of terms explaining the association between flow  $\tau$  and the factors is presented in equation (5) ( $R^2 = 96.78\%$ ). All the terms are highly significant ( $p < 0.0001$ ) except for  $SO$  ( $p = 0.001$ ),  $RBO$  ( $p = 0.001$ ),  $RBO \times SA$  ( $p = 0.002$ ), and  $SO \times RBO \times SA$  ( $p = 0.026$ ). The  $R^2(\text{adj})$  and  $R^2(\text{pred})$  were in good agreement (96.05% and 94.87% respectively).

$$\text{Flow } \tau = -6.763E+4 + 6.646E+4 \text{ SO} + 6.839E+4 \text{ RBO} + 1.965E+5 \text{ SO} \times \text{BW} + 1.211E+5 \text{ SO} \times \text{SA} + 1.687E+5 \text{ RBO} \times \text{BW} + 1.044E+5 \text{ RBO} \times \text{SA} + 2.260E+6 \text{ BW} \times \text{SA} - 4.633E+5 \text{ SO} \times \text{RBO} \times \text{BW} - 1.576E+5 \text{ SO} \times \text{RBO} \times \text{SA} - 4.539E+6 \text{ SO} \times \text{BW} \times \text{SA} - 4.408E+5 \text{ RBO} \times \text{BW} \times \text{SA} + 8.592E+6 \text{ SO} \times \text{RBO} \times \text{BW} \times \text{SA} \quad (5)$$

The best model created by backward elimination of terms to describe the association between flow  $\gamma$  and the factors is provided in equation (6) ( $R^2 = 68.88\%$ ). All the terms are highly significant ( $p < 0.0001$ ) except for  $RBO \times BW \times SA$  ( $p = 0.010$ ). The  $R^2(\text{adj})$  and  $R^2(\text{pred})$  were 67.02% and 65.33%, respectively.

$$\text{Flow } \gamma = -32.01 + 2287 \text{ SO} \times \text{RBO} \times \text{BW} + 3650 \text{ SO} \times \text{RBO} \times \text{SA} + 4040 \text{ RBO} \times \text{BW} \times \text{SA} - 34425 \text{ SO} \times \text{RBO} \times \text{BW} \times \text{SA} \quad (6)$$

The best model created by backward elimination of terms illustrating

the association between flow  $G'$  and the factors is given in equation (7) ( $R^2 = 95.44\%$ ). All the terms are highly significant ( $p < 0.0001$ ) in this model with the  $R^2(\text{adj})$  and  $R^2(\text{pred})$  values with good agreement (94.69% and 92.39% respectively).

$$\text{Flow } G' = -6.941\text{E}+3 - 4.383\text{E}+5 \text{ BW} + 5.636\text{E}+5 \text{ SO} \times \text{BW} - 8.699\text{E}+5 \text{ SO} \times \text{SA} + 6.107\text{E}+5 \text{ RBO} \times \text{BW} - 7.353\text{E}+5 \text{ RBO} \times \text{SA} + 3.965\text{E}+6 \text{ SO} \times \text{RBO} \times \text{SA} + 1.575\text{E}+7 \text{ SO} \times \text{BW} \times \text{SA} + 1.213\text{E}+7 \text{ RBO} \times \text{BW} \times \text{SA} - 6.603\text{E}+7 \text{ SO} \times \text{RBO} \times \text{BW} \times \text{SA} \quad (7)$$

Coefficient of determinations for all models explained above have the values above 90% (except for flow  $\gamma$ ) which indicates the adequacy of the model, and it can be concluded that the data obtained from this study is reliable for the optimization of the developed oleogel. ANOVA tables showed that all responses were significantly affected by the oils and oleogelators with  $R^2$  higher than 96% indicating the robustness of the model for the optimization.

**3.1.1.5. Contour plots.** Contour plots were created from the developed regression models (equations (2) to (7)) using Minitab 21.1. Regression model fitting is used to develop equations for each response to model the relationship between the response and all independent variables that have significant influence on the response, whereas contour plots are used to understand the influence of interaction effects among two different components (independent variables) on a response variable (Ghan et al., 2022). These plots are mainly used to develop visualizations (geometrical representation) of the relationship between the interaction effects of two components and the response. Fig. 1 shows the contour plots of different properties (responses) of oleogels against the combinations of oils and combinations of oleogelators. Crosshairs are randomly added in the figures in the desired range (similar to the commercial samples) of parameters. Crosshairs in the figures show the values of either oils or oleogelators as their amount in 1 g of the total mixture. Fig. 1 (A) and (B) show the relationship between the oil binding capacity and the oils and oleogelators, respectively. The oil binding capacity seems to be high (>90%) with different combinations of sesame oil and rice bran oil with sesame oil higher than 0.36 and rice bran oil higher than 0.41. That is, a higher proportion of rice bran oil than sesame oil in the mixture resulted in higher oil binding capacity.

From Fig. 1 (B), it is obvious that beeswax alone (at an amount higher than 0.12) was able to form a gel with an oil binding capacity higher than 95%, however, stearic acid was able to form gels with an oil binding capacity of above 95% at the amount higher than 0.01 when used together with beeswax higher than 0.08. Beeswax alone at the amount less than 0.10 and a combination of beeswax and stearic acid at the amount of 0.06 and 0.10 resulted in an oil binding capacity of less than 80%.

As indicated already in equation (3), the effect of the oils on the gel point was not highly significant, which is further evident by Fig. 1 (C). Crosshairs in Fig. 1 (C) and (D) show the range of oil combinations and oleogelator combinations that can yield a gel point between 50 and 55 °C, which is closer to the gel point of commercial margarine. The gel point of the oleogels increased with increasing the concentration of both oleogelators. This is in accordance with the results reported by Thakur et al. (2022) who demonstrated that the melting point of carnauba wax based oleogel was increased with increasing concentration of the carnauba wax.

Fig. 1 (E) and (F) show that the desired  $G'$  at LVR can be achieved over a narrow range of combinations of oil and oleogelators.  $G'$  at LVR is the most important property of the oleogel because it determines the strength of the oleogels. It indicates that optimization of the formulation using an optimization technique is necessary to find out the suitable mixture to obtain oleogel with desired properties.

Fig. 1 (G) and (H) show the effect of oils and oleogelators on flow  $\tau$ . Stearic acid with zero or very less amount of beeswax resulted in less values for the flow  $\tau$ , whereas beeswax alone (between 0.08 and 0.12)

and beeswax with less amount of stearic acid resulted in desirable values similar to commercial samples. Beeswax higher than 0.12 resulted in very high (>400) values. Flow  $\gamma$  and flow  $G'$  were mainly influenced by oleogelators (Fig. 1 (J) and (L)). Desired values for the flow  $\gamma$  and flow  $G'$  were obtained in narrow ranges of oleogelator concentrations.

### 3.2. Multi-response optimization

In order to determine the formula that can provide properties more similar to those of commercial samples, optimization was performed by setting the target values for the rheological properties and the maximum value (100%) for the oil binding capacity. The analysis of 4 different brands of commercial samples showed different values for the rheological properties. Therefore, the target value and the maximum and minimum values were adjusted to be closer to 4 samples. The optimization resulted in the following combination of mixtures: sesame oil = 0.40 g, rice bran oil = 0.48 g, beeswax = 0.09 g, and stearic acid = 0.03 g (sesame oil and rice bran oil at the ratio of 4:5 and beeswax and stearic acid at the ratio of 3:1 with a total oleogelator concentration of 11.74%).

Optimized oleogel was prepared in triplicates and analyzed to assure the validity of the model. The experimental results for the parameters were similar to the predicted values. Two controls were prepared to have either one of the oleogelator while maintaining the same total amount of oleogelator in order to find out if there is a synergistic effect of using a combination of beeswax and stearic acid as the oleogelators (control 1: sesame oil = 0.405 g, rice bran oil = 0.478 g, beeswax = 0.117 g and control 2: sesame oil = 0.405 g, rice bran oil = 0.478 g, and stearic acid = 0.117 g).

### 3.3. Characterization of optimized oleogel

The optimized oleogel and controls were analyzed for the oil binding capacity, rheological properties, thermal properties, microstructure, and molecular properties and compared with the properties of commercial margarine samples. Table 4 shows the oil binding capacity and rheological characteristics of the optimized oleogels and controls.

#### 3.3.1. Oil binding capacity

The oil binding capacities of the optimized oleogel and both controls were very high as shown in Table 4. However, the oil binding capacities of the commercial samples were much less (70–79%) compared to the oleogels. Ghan et al. (2022) also reported higher oil binding capacity (83.83%) of optimized oleogel developed using soy lecithin and glyceryl monostearate than the commercial spread. The reason for the lower oil binding capacity of the commercial samples could be the presence of water and other ingredients with the fat. More than 99% oil binding capacity of the oleogel samples shows that the strength of the gel network is enough to prevent oil leakage. The oil binding capacity of the oleogels reported in this study was in line with other researchers. Ögütçü et al. (2015) and Zbikowska et al. (2022) also reported the oil binding capacity of more than 99% for the oleogels developed using beeswax at concentrations ranging from 2 to 10%.

#### 3.3.2. Rheological properties

Optimized oleogel, controls, and reference samples were subjected to amplitude sweep, frequency sweep, temperature ramp, and thixotropy experiments using an oscillatory Rheometer (Anton Paar MCR302), and the data were analyzed using RheoCompass™ software. Amplitude sweep experiments were conducted to determine the LVR of the oleogels, followed by further characterization of oleogels using temperature ramp, frequency sweep, and thixotropy experiments. Temperature ramp experiments were performed to determine the behavior of oleogels with increasing temperature. A frequency sweep is used to investigate the long-term and short-term behavior of the sample at low and high frequencies, respectively. Three Interval Thixotropy Test (3 ITT) is a



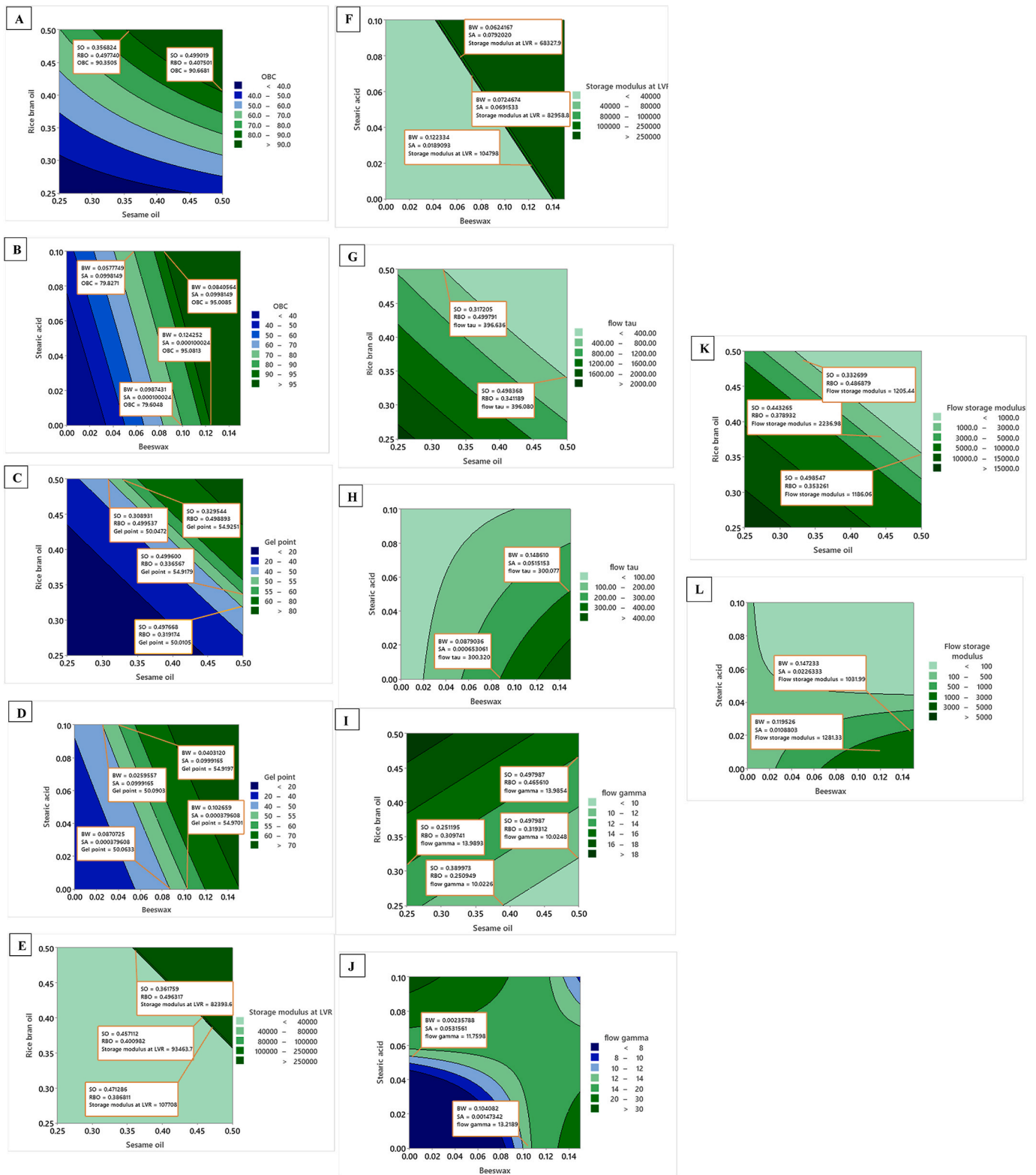


**Fig. 1.** Contour plots explaining the relationship between (A) oil binding capacity and rice bran oil and sesame oil, (B) oil binding capacity and stearic acid and beeswax, (C) gel point and rice bran oil and sesame oil, (D) gel point and stearic acid and beeswax, (E) flow  $G'$  and rice bran oil and sesame oil, (F) flow  $G'$  and stearic acid and beeswax, (G) flow  $\tau$  and rice bran oil and sesame oil (H) flow  $\tau$  and stearic acid and beeswax, (I) flow  $\gamma$  and rice bran oil and sesame oil, (J) flow  $\gamma$  and stearic acid and beeswax, (K)  $G'$  at LVR and rice bran oil and sesame oil, (L)  $G'$  at LVR and stearic acid and beeswax. All axis units are reported in g for the total mixture of 1 g.

**Table 4**  
A comparison of oil binding capacity and rheological properties of optimized oleogel and controls.

Parameter	Optimized oleogel	Control 1	Control 2	Reference
OBC (%)	99.99 ± 0.00 <sup>a</sup>	99.99 ± 0.00 <sup>a</sup>	98.43 ± 0.09 <sup>b</sup>	70.13–79.65 <sup>a</sup>
Gel point (°C)	62.63 ± 0.50 <sup>b</sup>	66.62 ± 0.58 <sup>a</sup>	51.81 ± 0.86 <sup>c</sup>	56.29–61.02 <sup>a</sup>
LVR limit	0.056 ± 0.002 <sup>a</sup>	0.048 ± 0.002 <sup>b</sup>	0.034 ± 0.003 <sup>c</sup>	0.022–0.034 <sup>a</sup>
G' at LVR (Pa)	108,000 ± 1,550 <sup>b</sup>	129,000 ± 3,530 <sup>a</sup>	6,070 ± 95.5 <sup>c</sup>	4,9300–7,8600 <sup>a</sup>
Loss factor	0.14 ± 0.003 <sup>b</sup>	0.15 ± 0.004 <sup>b</sup>	0.20 ± 0.004 <sup>a</sup>	0.14 ± 0.006 <sup>b</sup>
Flow τ (Pa)	217.15 ± 26.81 <sup>b</sup>	260 ± 8.77 <sup>a</sup>	38.29 ± 2.87 <sup>c</sup>	255.10–372.5 <sup>a</sup>
Flow γ (%)	12.17 ± 1.93 <sup>c</sup>	21.02 ± 1.19 <sup>b</sup>	46.88 ± 2.89 <sup>a</sup>	11.73–14.90 <sup>a</sup>
Flow G' (Pa)	1,180.67 ± 70.23 <sup>a</sup>	875.8 ± 20.65 <sup>b</sup>	57.85 ± 3.68 <sup>c</sup>	1,210–2,260 <sup>a</sup>
Structure recovery (%)	35.50 ± 2.96 <sup>b</sup>	30.57 ± 1.41 <sup>c</sup>	8.73 ± 0.75 <sup>d</sup>	53.33 ± 1.57 <sup>a</sup>

OBC: Oil binding capacity. Different superscript letters (a-d) in the same row show the significant difference ( $p < 0.05$ ).  
<sup>a</sup> Values for the references are provided as a range of values of four commercial samples.

rheological test carried out by subjecting the sample to alternating constant shear rates (0.1, 10, and 0.1 s<sup>-1</sup>) in three intervals (10, 5, and 10 min) and measuring the viscosity. Rheological parameters determined for the samples are shown in Table 4. Temperature ramp rheograms are presented in Fig. 2 and amplitude and frequency sweep rheograms are presented in Figs. 3 and 4., respectively. Fig. 5 shows the thixotropic rheograms of the samples.

An understanding of the thermal behavior of oleogels is important. Temperature ramp rheograms shown in Fig. 2 illustrate the changes in G'

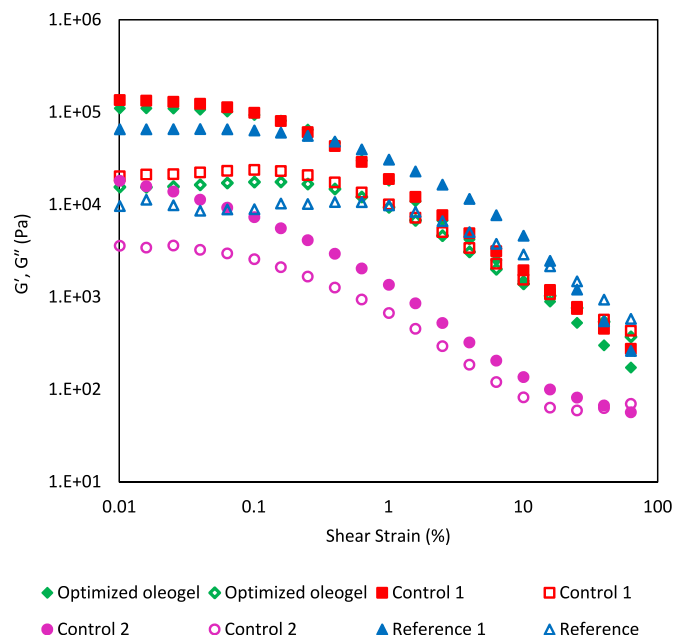


**Fig. 3.** Amplitude sweeps of optimized oleogel, controls, and reference sample. Closed series markers refer to the G' and open series markers refer to the G''.

and G'' during heating from 30 °C at the rate of 2 °C/min under constant strain and frequency. G' and G'' of all samples decreased with the increasing temperature which indicates gradual breakdown of the gel network, which is associated with a decline in elastic properties and a rise in viscous properties of the oleogel. With increasing temperature, at one point, complete loss of gelled state and crossover of G' and G'' occur, where G'' = G'. When the gel is transformed completely into liquid state, the sample exhibits viscous behaviour. The pattern of the behavior of the reference sample and the oleogels is different, however, the gel point of

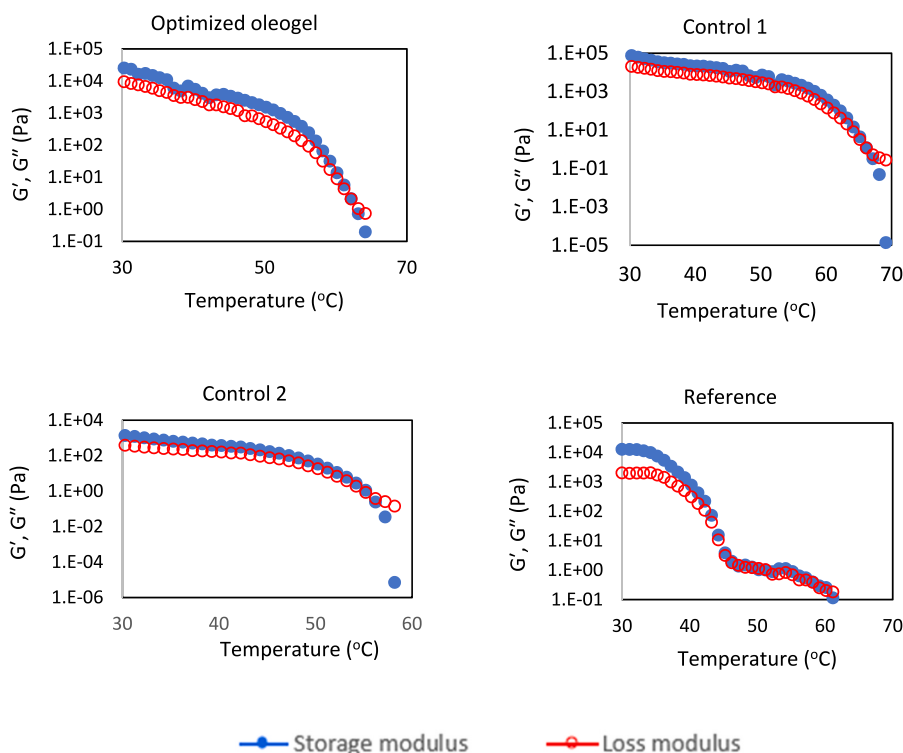


**Fig. 2.** Temperature ramps of properties of optimized oleogel, controls and reference sample.

the optimized oleogel and control 1 were not significantly different from the reference samples. The reference sample exhibited a sudden drop in both  $G'$  and  $G''$  with very closer values between 42 °C and 46 °C, that is, softening started at this point, however, there was no clear crossover point in this region. A clear crossover point was observed after 60 °C, which indicates the complete melting of the sample. The gel points of optimized oleogel and control 1 were not significantly different from that of the commercial sample, however control 2 had a significantly lowest gel point among all samples. The behavior of the gels with increasing temperature provides useful information about the spreadability of gels. Oleogels intended to prepare margarine should be spreadable at low temperature as it is stored in a refrigerator. However, at the same time, it should retain the structure without flowing at an elevated temperature, and to provide a good mouthfeel, it should have a soft solid structure at body temperature. According to Fig. 2., it is clear that the optimized oleogel and the reference would remain solid up to about 60 °C, however, the reference sample will start to melt at around 42 °C. The high melting point of optimized oleogel offers an advantage over the commercial sample that optimized oleogel would remain solid in the summer season with high temperatures without requiring refrigeration. The high gel point of oleogels has been considered as an advantage of oleogels by other researchers as well (Scharfe & Floter, 2020; Yilmaz & Demirci, 2021; Yilmaz et al., 2020).

Amplitude sweep experiment can be used to determine the strength of the gel using  $G'$  at LVR, loss factor, and LVR limit. At the LVR, all samples had higher  $G'$  than  $G''$  indicating the gel structure, which is in accordance with other studies (Naeli et al., 2022; Patel et al., 2015; Thakur et al., 2022). According to the data presented in Table 4, optimized oleogel exhibited a significantly longer LVR limit and higher  $G'$  at LVR than references and controls indicating a stronger gel network than the reference. A similar observation has been reported by Naeli et al. (2022). Compared to the reference, the optimized oleogel exhibited a less flow stress (flow  $\tau$ ) and  $G'$  but a similar flow strain (flow  $\gamma$ ). Thakur et al. (2022) also reported a similar value for the strain at flow point ( $12.01 \pm 0.2\%$ ), however, a higher stress value ( $361.4 \pm 0.6$  Pa) for the optimized oleogel based on carnauba wax (8%) and soybean oil than the value for the optimized oleogel reported in the present study.

The plateau value of  $G'$  in the LVR tells the rigidity of the sample and a longer LVR is evidence for the highest resistance against structure degradation. An ideal solid fat should have a  $G'$  ranging from  $1 \times 10^5$  to  $5 \times 10^6$  Pa and yield stress between 200 and 1000 Pa which covers the range 'soft' to 'hard' (Patel et al., 2020). Optimized oleogel had the  $G'$  within this range towards the 'soft' gel category. Control 1 had the highest  $G'$  whereas control 2 had the lowest even though all three oleogels were produced with the same amount of oleogelators. Therefore, it can be speculated that beeswax contributes to more elastic nature than stearic acid. This could be due to the superior gelling ability of the beeswax primarily attributed to the low polarity, long chain length, and high melting point of the components of the wax (Doan et al., 2015).

The loss factor ( $G''/G'$ ) is the ratio of energy dissipated in the material during vibrations to the maximum potential energy stored in the material (Zielonka & Dobkowski, 1998). A higher crossover point implies a stronger and more stable gel network (Doan et al., 2015; Tavernier et al., 2018). The optimized oleogel had significantly higher  $G'$  at the LVR than the commercial samples, however with similar loss factor values and crossover strain and slightly less  $G'$  at the flow point. The loss factor of optimized oleogel and control 1 were not significantly different from that of the commercial sample, whereas control 2 had a significantly higher loss factor indicating that control 2 had more viscous nature than other samples. The reference, optimized oleogel, and control 1 showed a sharp decrease in  $G'$  and  $G''$  at strain values higher than 1%. However, the sudden drop in  $G'$  and  $G''$  was less pronounced in the reference sample. Similar behavior (higher LVR, but a sudden drop in  $G'$  and  $G''$  compared to commercial shortenings) of the oleogel made from ethylcellulose/hydroxypropyl methylcellulose has also been reported (Naeli et al., 2022). These results indicate that, despite similar loss factor

and flow strain and higher LVR of optimized oleogel than the reference indicating the strong gel network, the optimized oleogel is more prone to structural deformation than the reference sample. On the other hand, a sudden drop in  $G'$  at high strain values denotes a good spreadability (Joyner, 2019) of the oleogel and this can be considered advantageous because this is a desirable property of margarines and spreads. Therefore, it can be concluded that optimized oleogel has better spreadability than the reference sample. When comparing the properties of optimized oleogel and the reference, overall, optimized oleogel exhibited similar or better properties as the reference sample in terms of strength of the gel network based on loss factor, LVR limit,  $G'$  at LVR and spreadability and oleogel flow at similar strain value, however, at slightly less  $G'$ .

Frequency sweep experiments are performed to study the time-dependent behavior of the gel in a non-destructive deformation range. For this purpose, the samples were subjected to a constant stress within LVR, and varying frequencies (0.01–100 Hz). Fig. 4 shows the frequency sweeps of the optimized oleogel, controls, and commercial margarine. All samples had higher  $G'$  than  $G''$  during the frequency sweep experiment indicating their elastic (solid-like) behavior. Based on the pattern of the  $G'$  with time and increasing frequency, the samples can be categorized into a strong gel (frequency independence) and weak gel (frequency dependent) (Tavernier et al., 2018). Strong gels will have constant  $G'$ , whereas weak gels will have increasing  $G'$  with increasing frequency. From Fig. 4., it is clear that the optimized oleogel and control 1 showed frequency-independent behavior until 10 Hz, and there was a slight increase in the  $G'$  afterward compared to the reference sample. The reference sample also showed a slight increase in the  $G'$ , however, the increase is less than the optimized oleogel and the control 1. The frequency dependency of the beeswax oleogel based margarines compared to the commercial margarine prepared using partially hydrogenated palm olein has also been reported by Abdolmaleki et al. (2022). The reason behind the observation in the present study and the observation by Abdolmaleki et al. (2022) clearly indicate that partially hydrogenated vegetable oils are less frequency dependent than beeswax based oleogels and therefore margarines prepared using beeswax based oleogels. Naeli et al. (2022) also reported an increase in  $G'$  and  $G''$  of the ethyl cellulose and hydroxypropyl methyl cellulose biopolymers based oleogels with increasing frequency. Control 2 showed an unstable pattern of  $G'$  indicating that the elasticity of the gel network is more dependent on frequency than other samples. Gómez-Estaca et al. (2019)

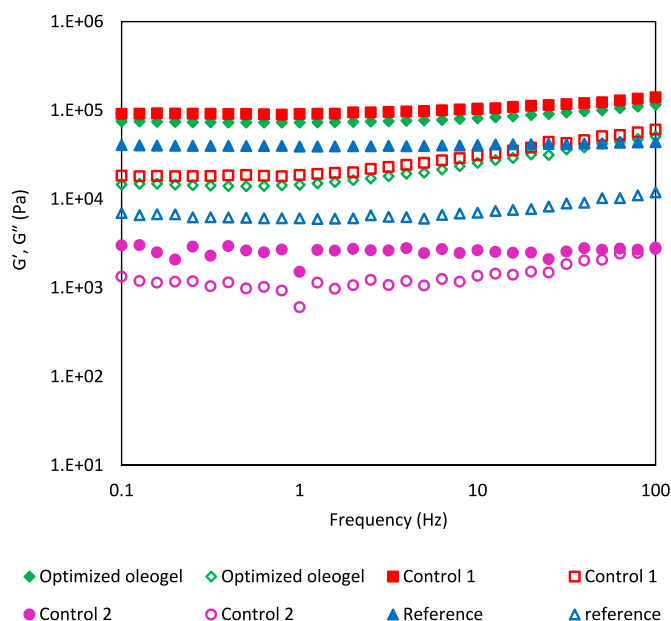


Fig. 4. Frequency sweeps of optimized oleogel, controls and reference sample. Closed series markers refer to the  $G'$  and open series markers refer to the  $G''$ .

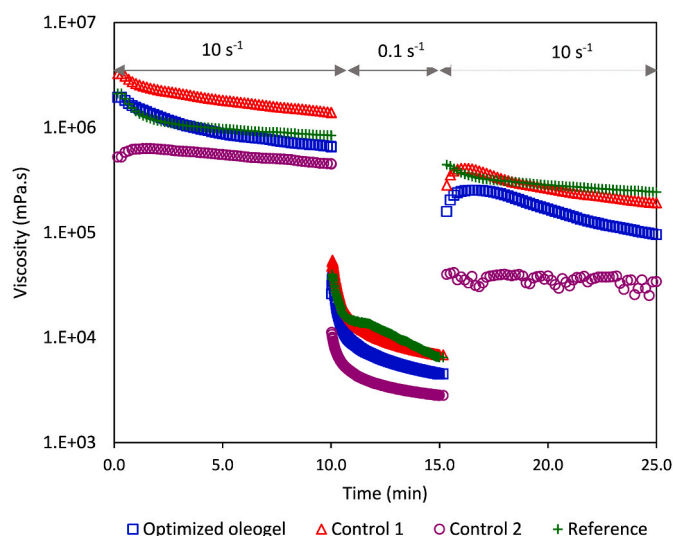


Fig. 5. Thixotropic properties of optimized oleogel, controls and reference sample.

also reported a similar behavior of beeswax based oleogel.

Thixotropy was used to examine the structure recovery ability of the oleogel samples after the application of shear. Evaluation of thixotropic behavior of oleogels is important if the oleogel is intended to be used in processing that involves mixing, whipping, and other mechanical breakdown operations. After the treatment, recovery of the gel network provides the functionalities of the solid fats (Yilmaz et al., 2021). Even though optimized oleogel had higher LVR limit, and higher  $G'$  at LVR than the references and the loss factor similar to the references, the structural recovery ability of the optimized oleogel was significantly less than the references. It indicates that even though the gel network is strong enough to hold the oil (as indicated by high oil binding capacity in section 3.3.1), the ability of the gel structure to withstand and recover the shear force is low. Despite beeswax based oleogels are rigid, the reason for the high sensitivity of beeswax based oleogel is that more deformation energy can be stored and at the same time more energy can be lost during shear (Gómez-Estaca et al., 2019). Patel et al. (2015) also reported that the gel networks formed by the natural waxes have high shear sensitivity and low thixotropic recovery.

Synergistic effects of oleogelators on oleogel properties indicates that the characteristics of an oleogel prepared using a combination of oleogelators are superior to their corresponding oleogel prepared using single oleogelator. Based on the rheological properties of optimized oleogel and controls, it can be concluded that beeswax and stearic acid had synergistic effects at the ratio of 3:1 on the rheological properties of oleogel. As shown in Table 4, the structural recovery, and LVR limit of optimized oleogel ( $35.50 \pm 2.96\%$ , and  $0.056 \pm 0.002$ , respectively) were significantly higher ( $p < 0.05$ ) than both control 1 ( $30.57 \pm 1.41\%$ , and  $0.048 \pm 0.002$ , respectively) and control 2 ( $8.73 \pm 0.75\%$ , and  $0.034 \pm 0.003$ , respectively). These results indicate that the oleogel made using the combination of oleogelators had superior structural characteristics compared to the oleogels made using single oleogelator at the same concentration. Many other authors also have reported the synergistic interactions among oleogelators based on the structural strength of the oleogels made from mixture of different oleogelators (Bin Sintang et al., 2017; Lopez-Martínez et al., 2015; Okuro et al., 2018; Tavernier et al., 2017; Winkler-Moser et al., 2019). The present study has reported the synergistic combination of beeswax and stearic acid for the first time because there are no previous studies reported on using the combination of beeswax and stearic acid. Therefore, the objective of this study has been fulfilled. This finding could be useful to develop oleogel with further improvements in the property to make it suitable for commercial applications.

### 3.3.3. Thermal properties

The thermal behavior of neat beeswax, stearic acid, and oleogels was determined by Netzsch DSC. The onset melting, peak melting, onset crystallization, peak crystallization, and enthalpy of melting and crystallization were evaluated using Netzsch Proteus® software. Fig. 6 shows the heating profile for the oleogel, oleogelators, and reference, and Table 5 shows the thermal properties of analyzed samples. The neat oleogelators and the oleogel samples exhibited distinct thermograms. The neat stearic acid had a melting and crystallization profile within a narrow range of temperatures ( $54\text{--}60\text{ }^{\circ}\text{C}$  and  $50\text{--}53\text{ }^{\circ}\text{C}$ , respectively). The neat beeswax exhibited broad melting and crystallization profiles ( $47\text{--}65\text{ }^{\circ}\text{C}$ , crystallization  $39$  to  $51$ ,  $^{\circ}\text{C}$  respectively). Broad melting and crystallization profiles of waxes are attributed to the multiple chemical components including hydrocarbons, fatty acids, fatty alcohols, and wax esters (Patel, 2015b). Ögütçü et al. (2015) also reported similar values for the melting temperatures of the beeswax. Contrary to the present study, Yi et al. (2017) have reported a lower value for the peak melting point of beeswax ( $42.25 \pm 0.22\text{ }^{\circ}\text{C}$ ) than reported in the present study. This difference could be due to the variations in the composition of wax from various suppliers. Melting and crystallization temperatures of stearic acid reported in this study agree with the results reported by Sagiri et al. (2015) for the neat stearic acid.

Optimized oleogel, control 1 and control 2 also exhibited broad melting profiles ( $34\text{--}53\text{ }^{\circ}\text{C}$ ,  $46\text{--}55\text{ }^{\circ}\text{C}$ , and  $29\text{--}45\text{ }^{\circ}\text{C}$ , respectively). However, the optimized oleogel and control 1 exhibited very broader exothermic peaks probably due to the heterogeneous chemical composition of the beeswax. Similar thermal behaviors have also been reported by Martins et al. (2016). Abdolmaleki et al. (2022) have reported that oleogel based on 10% of beeswax had a broad melting range of  $48\text{--}63\text{ }^{\circ}\text{C}$ . Peak melting and crystallization temperatures for the oleogel made using 16% of stearic acid from sesame oil ( $44.5\text{ }^{\circ}\text{C}$  and  $35.9\text{ }^{\circ}\text{C}$ , respectively) reported by Sagiri et al. (2015) were slightly higher than the values reported in the present study for the control 2, which was prepared using stearic acid as the only oleogelator. This could be due to the higher concentration of stearic acid than the concentration used in the present study for control 2. Crystallization was observed in a narrow range of temperatures for all three samples ( $46\text{--}48\text{ }^{\circ}\text{C}$  for the optimized oleogel,  $47\text{--}49\text{ }^{\circ}\text{C}$  for control 1, and  $31\text{--}34\text{ }^{\circ}\text{C}$  for control 2). Yi et al. (2017) also reported a narrow range of crystallization temperatures and broad range of temperature for melting of beeswax and carnauba wax based oleogels. The reference (market samples) showed multiple sharp

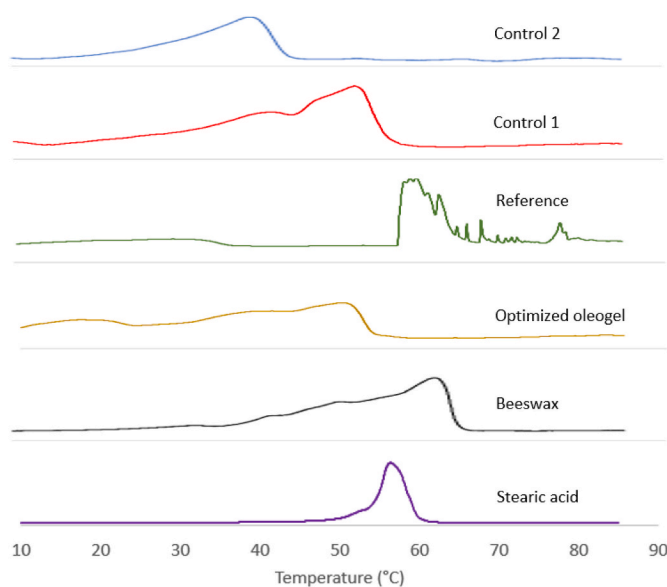


Fig. 6. DSC thermograms of melting for neat oleogelators, optimized oleogel, reference, and controls.

**Table 5**

Onset melting ( $T_{om}$ ), peak melting ( $T_{pm}$ ), onset crystallization ( $T_{oc}$ ), peak crystallization ( $T_{pc}$ ) and enthalpy of melting ( $\Delta H_m$ ), and crystallization ( $\Delta H_c$ ) of optimized oleogel, controls and references, and neat beeswax and stearic acid.

Sample	$T_{om}$ (°C)	$T_{pm}$ (°C)	$T_{oc}$ (°C)	$T_{pc}$ (°C)	$\Delta H_m$ (J/g)	$\Delta H_c$ (J/g)
Optimized oleogel	34.70 ± 0.71 <sup>c</sup>	50.33 ± 0.55 <sup>c</sup>	48.00 ± 0.53 <sup>d</sup>	47.40 ± 0.52 <sup>c</sup>	7.00 ± 0.39 <sup>d</sup>	-3.68 ± 0.55 <sup>c</sup>
Control 1	46.30 ± 0.14 <sup>b</sup>	51.60 ± 0.57 <sup>c</sup>	49.50 ± 0.35 <sup>c</sup>	48.65 ± 0.21 <sup>c</sup>	8.63 ± 1.66 <sup>d</sup>	-4.27 ± 0.52 <sup>c</sup>
Control 2	30.10 ± 2.46 <sup>c</sup>	40.80 ± 1.41 <sup>d</sup>	37.85 ± 0.21 <sup>e</sup>	34.20 ± 1.95 <sup>d</sup>	20.22 ± 2.59 <sup>c</sup>	-17.37 ± 2.51 <sup>c</sup>
Beeswax	48.87 ± 1.32 <sup>b</sup>	62.20 ± 0.56 <sup>a</sup>	61.23 ± 0.15 <sup>a</sup>	60.13 ± 0.60 <sup>a</sup>	162.75 ± 4.31 <sup>b</sup>	-136.70 ± 11.41 <sup>b</sup>
Stearic acid	54.30 ± 0.14 <sup>a</sup>	56.30 ± 0.14 <sup>b</sup>	53.30 ± 0.28 <sup>b</sup>	52.85 ± 0.07 <sup>b</sup>	173.65 ± 5.16 <sup>a</sup>	-174.95 ± 0.49 <sup>a</sup>
Reference	51.70-57.1 <sup>a</sup>	51.9-61.8 <sup>a</sup>	16.1-16.7 <sup>a</sup>	15.40-16.20 <sup>a</sup>	31.33-110.1 <sup>a</sup>	-1.80 to -2.63 <sup>a</sup>

$T_{om}$ : Onset melting,  $T_{pm}$ : peak melting,  $T_{oc}$ : onset crystallization,  $T_{pc}$ : peak crystallization,  $\Delta H_m$ : enthalpy of melting,  $\Delta H_c$ : enthalpy of crystallization.

Different superscript letters (a-e) in the same column show the significant difference ( $p < 0.05$ ).

<sup>a</sup> Values for the references are provided as a range of values of four commercial samples.

exothermic peaks in the temperature range of 52–62 °C and a less crystallization temperature (14–17 °C) compared to all other samples.

The oleogels exhibited lower onset and peak melting and crystallization temperatures and enthalpies than the neat oleogelators. The reason behind the lower onset and peak temperatures of oleogel than the neat oleogelators could be the dilution effect of oleogelator constituents in the oil (Barroso et al., 2020; Doan et al., 2017) and the interaction between the moieties in the oleogelators and the oil. Doan et al. (2017) have explained that the presence of fatty acid fractions in plant waxes could interfere with the crystallization of the wax esters. Similarly, it could be explained that there may be interactions between the minor components and the fatty acids in the oils with the moieties present in the oleogelators and these interactions could influence the melting and crystallization. Even though the neat stearic acid exhibited a narrow range of temperatures for melting and crystallization, the oleogel made with stearic acid as the only oleogelator (control 2) showed an extended range of temperatures for melting. This could be due to the reason that the process of gel-to-sol transition is a continuous process and not an immediate process (Sagiri et al., 2015). Another notable difference among the thermograms of oleogelators is that the heating curves of optimized oleogel and control 1 showed a shoulder before the highest peak which is absent in control 2. The presence of shoulders in optimized oleogel and control 1 could be attributed to the multiple chemical components in the beeswax.

Ögütçü et al. (2015) have reported the peak melting temperature of neat beeswax and oleogel made using 3% of beeswax from cod liver oil as 63.15 °C and 45.42 °C, respectively. This peak melting temperature of the neat beeswax agrees with the value reported in the present study (Table 5). The onset of melting and crystallization and enthalpy of melting and crystallization of optimized oleogels also agree with the values reported by Martins et al. (2016) for the beeswax oleogels made from medium-chain triacylglycerols and long-chain triacylglycerols. Melting temperatures increase with increasing concentrations of the oleogelators (Suriaini et al., 2023; Thakur et al., 2022). This is in agreement with the higher melting temperature of the optimized oleogel (which is prepared using 9% of beeswax and 3% of stearic acid) reported in this study than the temperature reported by Ögütçü et al. (2015). Patel (2015b) has reported lower values for the onset of crystallization and peak crystallization temperatures (42.69 ± 0.35 °C and 40.98 ± 0.75 °C, respectively), for the beeswax based oleogel in high oleic sunflower oil than the values reported in the present study. This could be ascribed to the variations in the composition, viscosity, and polarity of the oils. Yang et al. (2018) reported different temperatures of crystallization and enthalpies for the oleogels made from different oils such as extra virgin olive oil, corn oil, sunflower oil and flaxseed oil using the same mixture of  $\beta$ -sitosterol and stearic acid at the same concentration.

### 3.3.4. Oxidation behavior

Oxidation induction time is the time interval between the initiation of oxygen or airflow and the onset of the oxidation reaction. The oxidation induction temperature is the temperature of the onset of the oxidation reaction. Oxidation induction time and oxidation induction

temperature of the oleogels, oils, and reference samples were determined by heating the samples from 30 to 700 °C at a constant heating rate (non-isothermal) of 20 °C per min, in a simultaneous thermal analyzer. The higher the oxidation induction time and temperature, the higher the stability of the sample against oxidation. The induction time and temperature were identified by the Netzsch Proteus software from the mass loss of the sample.

The sesame oil had the highest stability against oxidation (15.3 min, 340.2 °C) followed by rice bran oil (15 min, 333.0 °C). All oleogel samples had significantly lower oxidation stabilities (optimized oleogel: 14.7 min, 328.0 °C; control 1: 14.6 min, 324.7 °C and control 2: 14.6 min, 323.9 °C), however, higher than the reference sample (14 min, 312.4 °C). Ögütçü et al. (2015) also reported that the oxidative stability of the oleogel based on waxes without any added antioxidants is not good enough for commercial applications. Therefore, it is strongly suggested to improve the oxidative stability of the oleogels by adding antioxidants.

### 3.3.5. Microstructure

Crystal arrangement and crystal morphology of the oleogels were studied using polarized light microscopy to understand the effect of oleogelators and the combination of oleogelators on oleogel properties. Polarized light microscopy images of optimized formulation, controls, and reference samples are shown in Fig. 7. The oleogel prepared using only beeswax (control 1) contained needle-like crystals. Needle-like crystals have been reported by many researchers for the oleogels prepared using beeswax (Li et al., 2022; Patel, 2015b; Scharfe et al., 2022; Suriaini et al., 2023; Winkler-Moser et al., 2019; Zbikowska et al., 2022). The needle shape appearance could be the 2D perspective of platelet crystals as confirmed through scanning electron microscopy by Blake and Marangoni (2015b). The optimized oleogels contained needle-like crystals similar to that appeared in control 1 with bright areas of agglomerates of size varying from 100 to 300  $\mu$ m. Similar observations were reported for the oleogels made using combinations of oleogelators in other studies (Suriaini et al., 2023; Winkler-Moser et al., 2019). Similarly, Scharfe et al. (2022) also reported similar large spherulitic crystal arrangements among a finely distributed mesh of small crystals in the oleogel made using rice bran wax, and the authors could not clearly interpret it. The reference sample also had large agglomerates of spherulitic crystals of varying sizes distributed randomly. The appearance of agglomerates/aggregates in the optimized oleogels shows the similarity between the optimized oleogel and the reference.

The oleogel prepared using only stearic acid (control 2) contained fiber-like crystals in aggregates with continuous branching. This is in agreement with the appearance of stearic acid crystals in oleogels by other researchers (Gaudino et al., 2019; Sagiri et al., 2015; Wei et al., 2021). Generally, low molecular weight oleogelators form fibrous gel structures via self-assembly of molecules by non-covalent interactions. Thin self-assembled fibers orient into fibrillar bundles (Sagiri et al., 2015). Fibrillar bundles/aggregates can be clearly seen in the stearic acid oleogel in Fig. 7 (C).

Compared to the sizes of the crystals in both controls, the optimized

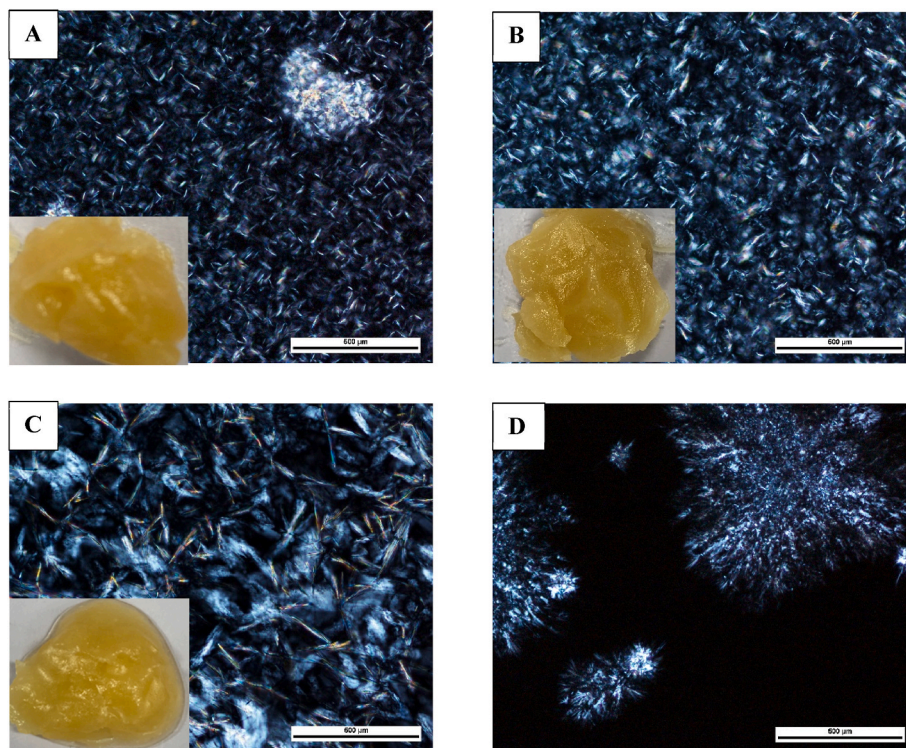


Fig. 7. Polarized microscopy images of optimized oleogel (A), control 1 (B), control 2 (C) and reference (D). Images were acquired at magnification  $200\times$  at  $20^\circ\text{C}$ . Scale bar:  $600\ \mu\text{m}$ .

oleogel prepared using both beeswax and stearic acid showed denser and smaller crystals which indicate the interaction among both oleogelators and the hardening of the network. A similar observation was reported by Li et al. (2022) when monoglyceride and wax are used in combinations in high oleic sunflower oil oleogel. Less prominent fibrous crystals in the optimized oleogel could be due to the less proportion of stearic acid to beeswax and the visualization of the fibrous crystals may be hindered by the birefringence of beeswax crystals. The size of crystals in optimized oleogel and control 1 are much smaller than the size of crystals in control 2 despite the fact that all oleogels were prepared using the same concentration of oleogelators. Wei et al. (2021) also reported the similar observation for the beeswax and stearic acid based oleogels prepared using same concentration of oleogelators. Small and dense crystals are associated with high oil binding capacity (Blake & Marangoni, 2015a). Therefore, differences in the size and arrangement of the beeswax and stearic acid crystals could be the reason for the differences on the oil binding capacities of optimized oleogel and controls.

Needle-like crystals are beneficial in gel formation because they are considered to connect the interfaces of the network and thus increase the oil holding capacity of the oleogel (Dassanayake et al., 2012; Li et al., 2022; Suriaini et al., 2023). Similarly, in the present study, optimized oleogel and control 1, which contained needle-like crystals, exhibited higher oil binding capacities and better rheological properties than control 2.

### 3.3.6. Molecular properties

The molecular interactions between oleogelators and the oils were explored using FTIR spectroscopy. Fig. 8 shows the FTIR spectra of the oils, oleogelators, oleogels, and reference samples. In the functional group region of the spectra, three prominent peaks in the regions of  $1695\text{--}1742\ \text{cm}^{-1}$  (carbonyl group),  $2846\text{--}2853\ \text{cm}^{-1}$  (asymmetric  $\text{CH}_2$  stretching), and  $2919\text{--}2922\ \text{cm}^{-1}$  (symmetric  $\text{CH}_2$  stretching) and two less prominent peaks in the regions of  $2942\text{--}2953\ \text{cm}^{-1}$  (alkyl C-H stretching) and  $3004\text{--}3006\ \text{cm}^{-1}$  (alkenyl C-H stretching) were identified. There were no peaks identified in the regions of  $3400\text{--}3550\ \text{cm}^{-1}$

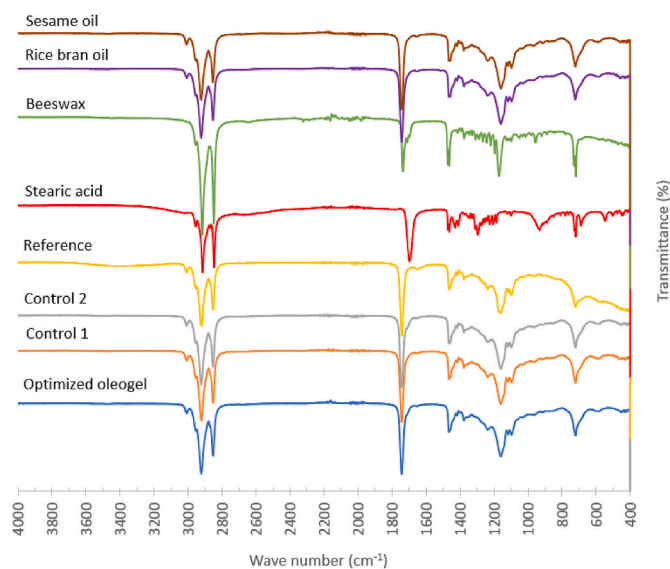


Fig. 8. FTIR spectra of oils, neat oleogelators, oleogels and reference.

indicating that there is no hydrogen bonding involved in any of the samples including the commercial sample. Similarly, no absorbance in the region corresponding to hydrogen bonds was not reported in the FTIR spectra of beeswax oleogels made from different oil phases (Fayaz et al., 2017; Gómez-Estaca et al., 2019; Martins et al., 2016; Yılmaz & Ögütçü, 2014). In contrary, peaks corresponding to the O-H stretching have been reported in the literature for the oleogels prepared using monoglycerides (Li et al., 2022; Lupi et al., 2016, 2017).

The  $\text{CH}_2$  stretching peaks appeared at  $2920.711\ \text{cm}^{-1}$  and  $2852.731\ \text{cm}^{-1}$  for the sesame oil and  $2922.157\ \text{cm}^{-1}$  and  $2851.767\ \text{cm}^{-1}$  for the rice bran oil, whereas the same peaks appeared at lower wave numbers

such as 2915.89  $\text{cm}^{-1}$  and 2847.91  $\text{cm}^{-1}$  for the beeswax and 2913.479  $\text{cm}^{-1}$  and 2846.946  $\text{cm}^{-1}$  for the stearic acid. The corresponding  $\text{CH}_2$  stretching peaks appeared at 2921.193 and 2851.285 for the optimized oleogel, 2919.747 and 2850.803 for the control 1 and 2920.711 and 2850.803 for control 2. Li et al. (2022) explained the similar slight shifts in the peaks that are characteristic of the  $\text{CH}_2$  stretching vibration is due to the change in the fluidity of the alkyl chain due to van der Waals forces.

The peaks assigned for the C–H stretching of alkene (C=C) appeared between 3004.118  $\text{cm}^{-1}$  and 3006.047  $\text{cm}^{-1}$  in the oils, oleogels, and commercial samples and did not appear for both beeswax and stearic acid. Optimized oleogels as well as controls showed similar peaks as the commercial sample with only a slight difference in the wavenumbers of the peaks except in the fingerprint region (400  $\text{cm}^{-1}$  and 1500  $\text{cm}^{-1}$ ) which is unique to the particular compound indicating similar molecular interactions.

Despite slight shifts in the peaks, there were no new peaks or disappearance of peaks occurred in the oleogels indicating clearly that the gel network is formed only via physical interactions, especially, van der Waals forces. These observations agree with the results reported by numerous other researchers. Li et al. (2022) and Gómez-Estaca et al. (2019) have concluded that the formation of a gel network in beeswax based oleogel is primarily via van der Waals interactions. Martins et al. (2016) also reported that there were no peak formation or peak disappearance, or peak shifts observed for the oleogels made from different oil phases using beeswax. From these findings and interpretations, it can be speculated that van der Waals forces govern the gel network formation in beeswax and stearic acid based oleogels.

#### 4. Conclusion

This study focused on optimization of the development of oleogel from sesame oil and rice bran oil using beeswax and stearic acid as oleogelators. Multi-response optimization of the mixture was successfully performed by Extreme Vertices Design. The data fitted the model with insignificant lack of fit values and high coefficient values for all the responses except for flow  $\gamma$ . Beeswax and stearic acid exhibited synergistic effects at the ratio of 3:1. The properties of optimized oleogel were determined and compared with those of commercial margarine samples. Optimized oleogel had a very high oil binding capacity (99.99%) indicating a very strong gel network. When comparing the properties of optimized oleogel and commercial margarines, optimized oleogel exhibited similar or better properties as the reference sample in terms of strength of the gel network based on loss factor, LVR limit,  $G'$  at LVR and spreadability, and oleogel flow at similar strain value, however, with slightly less  $G'$ . Overall, optimized oleogels had the similar rheological properties except for the structure recovery ability. The DSC analysis showed that the optimized oleogel had a melting point of  $50.33 \pm 0.55$  °C. FTIR analysis of the oleogels showed that the network structure has been formed by the physical entanglements and without any chemical alteration to the oils. Compared to the commercial margarine, optimized oleogel had higher stability against oxidation, however less than the oils. In conclusion, the mechanical and thermal properties of the optimized oleogel indicate that the oleogel possesses many characteristics suitable for making margarines. Further studies will be oriented to enhance the structural recovery ability and oxidative stability of the optimized oleogel via modifying processing conditions and incorporation of natural antioxidants.

#### Author declaration

The authors declare that this is an original research and the manuscript has not been submitted to any other journal. All the author have made significant contributions in the concept development, experiments, analysis, manuscript drafting and reviewing and editing of the paper.

#### Declaration of competing interest

We like to declare that the authors have no conflict of interest.

#### Data availability

Data will be made available on request.

#### Acknowledgements

This work was financially supported by Queensland University of Technology (QUT), Australia and Accelerating Higher Education Expansion and Development (AHEAD) - a World Bank-funded Sri Lankan government operation. The authors would like to acknowledge the laboratory facilities from the Central Analytical Research Facility (CARF) and the Centre for Agriculture and the Bioeconomy (CAB) of Queensland University of Technology (QUT), Australia, and the Research and Training Complex of the Faculty of Agriculture, University of Jaffna, Sri Lanka.

#### References

- Abdolmaleki, K., Alizadeh, L., Nayebzadeh, K., Baranowska, H. M., Kowalczewski, P.L., & Mousavi Khaneghah, A. (2022). Potential application of hydrocolloid-based oleogel and beeswax oleogel as partial substitutes of solid fat in margarine. *Applied Sciences*, 12(23). <https://doi.org/10.3390/app122312136>
- Abdolmaleki, K., Alizadeh, L., Nayebzadeh, K., Hosseini, S. M., & Shahin, R. (2020). Oleogel production based on binary and ternary mixtures of sodium caseinate, xanthan gum, and guar gum: Optimization of hydrocolloids concentration and drying method. *Journal of Texture Studies*, 51(2), 290–299. <https://doi.org/10.1111/jtxs.12469>
- Aguilar-Zárte, M., Macias-Rodríguez, B. A., Toro-Vazquez, J. F., & Marangoni, A. G. (2019). Engineering rheological properties of edible oleogels with ethylcellulose and lecithin. *Carbohydrate Polymers*, 205, 98–105. <https://doi.org/10.1016/j.carbpol.2018.10.032>
- Alizadeh, L., Abdolmaleki, K., Nayebzadeh, K., & Hosseini, S. M. (2020). Oleogel fabrication based on sodium caseinate, hydroxypropyl methylcellulose, and beeswax: Effect of concentration, oleogelation method, and their optimization. *Journal of the American Oil Chemists' Society*, 97(5), 485–496. <https://doi.org/10.1002/aocs.12341>
- Barroso, N. G., Okuro, P. K., Ribeiro, A. P. B., & Cunha, R. L. (2020). Tailoring properties of mixed-component oleogels: Wax and monoglyceride interactions towards flaxseed oil structuring. *Gels (Basel, Switzerland)*, 6(1), 5. <https://doi.org/10.3390/gels6010005>
- Bin Sintang, M. D., Danthine, S., Brown, A., Van de Walle, D., Patel, A. R., Tavernier, I., Rimaux, T., & Dewettinck, K. (2017). Phytosterols-induced viscoelasticity of oleogels prepared by using monoglycerides. *Food Research International*, 100, 832–840. <https://doi.org/10.1016/j.foodres.2017.07.079>
- Blake, A. I., & Marangoni, A. G. (2015a). The effect of shear on the microstructure and oil binding capacity of wax crystal networks. *Food Biophysics*, 10(4), 403–415. <https://doi.org/10.1007/s11483-015-9398-z>
- Blake, A. I., & Marangoni, A. G. (2015b). Plant wax crystals display platelet-like morphology. *Food Structure*, 3, 30–34. <https://doi.org/10.1016/j.foosr.2015.01.001>
- Co, E. D., & Marangoni, A. G. (2012). Organogels: An alternative edible oil-structuring method. *Journal of the American Oil Chemists' Society*, 89(5), 749–780. <https://doi.org/10.1007/s11746-012-2049-3>
- Dassanayake, L. S., Kodali, D. R., Ueno, S., & Sato, K. (2012). Crystallization kinetics of organogels prepared by rice bran wax and vegetable oils. *Journal of Oleo Science*, 61(1), 1–9. <https://doi.org/10.5650/jos.61.1>
- Doan, C. D., To, C. M., De Vrieze, M., Lynen, F., Danthine, S., Brown, A., Dewettinck, K., & Patel, A. R. (2017). Chemical profiling of the major components in natural waxes to elucidate their role in liquid oil structuring. *Food Chemistry*, 214, 717–725. <https://doi.org/10.1016/j.foodchem.2016.07.123>
- Doan, C. D., Van de Walle, D., Dewettinck, K., & Patel, A. R. (2015). Evaluating the oil-gelling properties of natural waxes in rice bran oil: Rheological, thermal, and microstructural study [10.1007/s11746-015-2645-0]. *Journal of the American Oil Chemists' Society*, 92(6), 801–811. <https://doi.org/10.1007/s11746-015-2645-0>
- Fayaz, G., Calligaris, S., & Nicoli, M. C. (2020). Comparative study on the ability of different oleogelators to structure sunflower oil [Article]. *Food Biophysics*, 15(1), 42–49. <https://doi.org/10.1007/s11483-019-09597-9>
- Fayaz, G., Goli, S. A. H., Kadivar, M., Valoppi, F., Barba, L., Balducci, C., Conte, L., Calligaris, S., & Nicoli, M. C. (2017). Pomegranate seed oil organogels structured by propolis wax, beeswax, and their mixture [10.1002/ejlt.201700032]. *European Journal of Lipid Science and Technology*, 119(10), Article 1700032. <https://doi.org/10.1002/ejlt.201700032>
- Flöter, E., Wettlaufer, T., Conty, V., & Scharfe, M. (2021). Oleogels-Their applicability and methods of characterization. *Molecules*, 26(6), 1673. <https://doi.org/10.3390/molecules26061673>

- Gaudio, N., Ghazani, S. M., Clark, S., Marangoni, A. G., & Acevedo, N. C. (2019). Development of lecithin and stearic acid based oleogels and oleogel emulsions for edible semisolid applications. *Food Research International*, 116, 79–89. <https://doi.org/10.1016/j.foodres.2018.12.021>
- Ghan, S. Y., Siow, L. F., Tan, C. P., Cheong, K. W., & Thoo, Y. Y. (2022). Palm olein organogelation using mixtures of soy lecithin and glyceryl monostearate. *Gels (Basel, Switzerland)*, 8(1).
- Gómez-Estaca, J., Herrero, A. M., Herranz, B., Álvarez, M. D., Jiménez-Colmenero, F., & Cofrades, S. (2019). Characterization of ethyl cellulose and beeswax oleogels and their suitability as fat replacers in healthier lipid pâtés development. *Food Hydrocolloids*, 87, 960–969. <https://doi.org/10.1016/j.foodhyd.2018.09.029>
- Guo, S., Song, M., Gao, X., Dong, L., Hou, T., Lin, X., Tan, W., Cao, Y., Rogers, M., & Lan, Y. (2020). Assembly pattern of multicomponent supramolecular oleogel composed of ceramide and lecithin in sunflower oil: Self-assembly or self-sorting? *Food & Function*, 11(9), 7651–7660. <https://doi.org/10.1039/d0fo00635a>
- Han, W. J., Chai, X. H., Liu, Y. F., Xu, Y. J., & Tan, C. P. (2022). Crystal network structure and stability of beeswax-based oleogels with different polyunsaturated fatty acid oils. *Food Chemistry*, 381. <https://doi.org/10.1016/j.foodchem.2021.131745>. Article 131745.
- Hunter, J. E., Zhang, J., & Kris-Etherton, P. M. (2010). Cardiovascular disease risk of dietary stearic acid compared with trans, other saturated, and unsaturated fatty acids: A systematic review. *The American Journal of Clinical Nutrition*, 91(1), 46–63. <https://doi.org/10.3945/ajcn.2009.27661>
- Jayaraj, P., Narasimulu, C. A., Rajagopalan, S., Parthasarathy, S., & Desikan, R. (2020). Sesamol: A powerful functional food ingredient from sesame oil for cardioprotection. *Food & Function*, 11(2), 1198–1210. <https://doi.org/10.1039/c9fo01873e>
- Joyner, H. S. (2019). *Rheology of semisolid foods*. Springer Cham. <https://doi.org/10.1007/978-3-030-27134-3>
- Liang, Y., Gao, Y., Lin, Q., Luo, F., Wu, W., Lu, Q., & Liu, Y. (2014). A review of the research progress on the bioactive ingredients and physiological activities of rice bran oil. *European Food Research and Technology*, 238(2), 169–176. <https://doi.org/10.1007/s00217-013-2149-9>
- Li, J., Guo, R., Wang, M., Bi, Y., Zhang, H., & Xu, X. (2022). Development and characterization of compound oleogels based on monoglycerides and edible waxes. *ACS Food Science & Technology*, 2(2), 302–314. <https://doi.org/10.1021/acsfodsctech.1c00390>
- Lopez-Martínez, A., Charó-Alonso, M. A., Marangoni, A. G., & Toro-Vazquez, J. F. (2015). Monoglyceride organogels developed in vegetable oil with and without ethylcellulose. *Food Research International*, 72, 37–46. <https://doi.org/10.1016/j.foodres.2015.03.019>
- Lupi, F. R., Greco, V., Baldino, N., de Cindio, B., Fischer, P., & Gabriele, D. (2016). The effects of intermolecular interactions on the physical properties of organogels in edible oils. *Journal of Colloid and Interface Science*, 483, 154–164. <https://doi.org/10.1016/j.jcis.2016.08.009>
- Lupi, F. R., Shakeel, A., Greco, V., Baldino, N., Calabrò, V., & Gabriele, D. (2017). Organogelation of extra virgin olive oil with fatty alcohols, glyceryl stearate and their mixture. *Lebensmittel-Wissenschaft & Technologie*, 77, 422–429. <https://doi.org/10.1016/j.lwt.2016.11.082>
- Martins, A. J., Cerqueira, M. A., Fasolin, L. H., Cunha, R. L., & Vicente, A. A. (2016). Beeswax organogels: Influence of gelator concentration and oil type in the gelation process. *Food Research International*, 84, 170–179. <https://doi.org/10.1016/j.foodres.2016.03.035>
- Naeli, M. H., Milani, J. M., Farmani, J., & Zargaran, A. (2022). Developing and optimizing low-saturated oleogel shortening based on ethyl cellulose and hydroxypropyl methyl cellulose biopolymers. *Food Chemistry*, 369. <https://doi.org/10.1016/j.foodchem.2021.130963>. Article 130963.
- Ögütçü, M., Arifoğlu, N., & Yılmaz, E. (2015). Storage stability of cod liver oil organogels formed with beeswax and carnauba wax [10.1111/ijfs.12612]. *International Journal of Food Science and Technology*, 50(2), 404–412. <https://doi.org/10.1111/ijfs.12612>
- Oh, I. K., Amoah, C., Lim, J., Jeong, S., & Lee, S. (2017). Assessing the effectiveness of wax-based sunflower oil oleogels in cakes as a shortening replacer. *Lebensmittel-Wissenschaft & Technologie*, 86, 430–437. <https://doi.org/10.1016/j.lwt.2017.08.021>
- Okuro, P. K., Santos, T. P., & Cunha, R. L. (2021). Compositional and structural aspects of hydro- and oleogels: Similarities and specificities from the perspective of digestibility. *Trends in Food Science & Technology*, 111, 55–67. <https://doi.org/10.1016/j.tifs.2021.02.053>
- Okuro, P. K., Tavernier, I., Bin Sintang, M. D., Skirtach, A. G., Vicente, A. A., Dewettinck, K., & Cunha, R. L. (2018). Synergistic interactions between lecithin and fruit wax in oleogel formation. *Food Funct*, 9(3), 1755–1767. <https://doi.org/10.1039/c7fo01775h>
- Palla, C., Giacomozzi, A., Genovese, D. B., & Carrín, M. E. (2017). Multi-objective optimization of high oleic sunflower oil and monoglycerides oleogels: Searching for rheological and textural properties similar to margarine. *Food Structure*, 12, 1–14. <https://doi.org/10.1016/j.foosr.2017.02.005>
- Patel, A. R. (2015a). *Alternative routes to oil structuring* (1 ed.). Springer International Publishing. <https://doi.org/10.1007/978-3-319-19138-6>
- Patel, A. R. (2015b). Natural waxes as oil structurants. In A. R. Patel (Ed.), *Alternative routes to oil structuring* (pp. 15–27). Springer International Publishing. [https://doi.org/10.1007/978-3-319-19138-6\\_2](https://doi.org/10.1007/978-3-319-19138-6_2)
- Patel, A. R. (2017). A colloidal gel perspective for understanding oleogelation. *Current Opinion in Food Science*, 15, 1–7. <https://doi.org/10.1016/j.cofs.2017.02.013>
- Patel, A. R. (2018). Oil Structuring: Concepts, overview and future perspectives. In *Edible oil structuring: Concepts, methods and applications* (pp. 1–22). The Royal Society of Chemistry. <https://doi.org/10.1039/9781788010184-00001>
- Patel, A. R., Babaahmadi, M., Lesaffer, A., & Dewettinck, K. (2015). Rheological profiling of organogels prepared at critical gelling concentrations of natural waxes in a triacylglycerol solvent. *Journal of Agricultural and Food Chemistry*, 63(19), 4862–4869. <https://doi.org/10.1021/acs.jafc.5b01548>
- Patel, A. R., & Dewettinck, K. (2015). Comparative evaluation of structured oil systems: Shellac oleogel, HPMC oleogel, and HIPE gel [10.1002/ejlt.201400553]. *European Journal of Lipid Science and Technology*, 117(11), 1772–1781. <https://doi.org/10.1002/ejlt.201400553>
- Patel, A. R., Nicholson, R. A., & Marangoni, A. G. (2020). Applications of fat mimetics for the replacement of saturated and hydrogenated fat in food products. *Current Opinion in Food Science*, 33, 61–68. <https://doi.org/10.1016/j.cofs.2019.12.008>
- Punia, S., Kumar, M., Sandhu, K. S., & Whiteside, W. S. (2021). Rice-bran oil: An emerging source of functional oil. *Journal of Food Processing and Preservation*, 45(4), Article e15318. <https://doi.org/10.1111/jfpp.15318>
- Sagiri, S. S., Singh, V. K., Pal, K., Banerjee, I., & Basak, P. (2015). Stearic acid based oleogels: A study on the molecular, thermal and mechanical properties. *Materials Science and Engineering: C*, 48, 688–699. <https://doi.org/10.1016/j.msec.2014.12.018>
- Scharfe, M., & Floter, E. (2020). Oleogelation: From scientific feasibility to applicability in food products. *European Journal of Lipid Science and Technology*, 122(12), Article 2000213. <https://doi.org/10.1002/ejlt.202000213>
- Scharfe, M., Niksch, J., & Flöter, E. (2022). Influence of minor oil components on sunflower, rice bran, candellilla, and beeswax oleogels [10.1002/ejlt.202100068]. *European Journal of Lipid Science and Technology*, 124(7), Article 2100068. <https://doi.org/10.1002/ejlt.202100068>
- Sintang, M. D. B., Rimaux, T., Van de Walle, D., Dewettinck, K., & Patel, A. R. (2017). Oil structuring properties of monoglycerides and phytosterols mixtures. *European Journal of Lipid Science and Technology*, 119(3), Article 1500517. <https://doi.org/10.1002/ejlt.201500517>
- Suriani, N., Arpi, N., Syamsuddin, Y., & Supardan, M. D. (2023). Characteristics of palm oil-based oleogel and its potency as a shortening replacer. *South African Journal of Chemical Engineering*, 43, 197–203. <https://doi.org/10.1016/j.sajce.2022.11.003>
- Tavernier, I., Doan, C. D., Van der Meeren, P., Heyman, B., & Dewettinck, K. (2018). The potential of waxes to alter the microstructural properties of emulsion-templated oleogels [10.1002/ejlt.201700393]. *European Journal of Lipid Science and Technology*, 120(3), Article 1700393. <https://doi.org/10.1002/ejlt.201700393>
- Tavernier, I., Doan, C. D., Van de Walle, D., Danthine, S., Rimaux, T., & Dewettinck, K. (2017). Sequential crystallization of high and low melting waxes to improve oil structuring in wax-based oleogels [10.1039/C6RA27650D]. *RSC Advances*, 7(20), 12113–12125. <https://doi.org/10.1039/C6RA27650D>
- Thakur, D., Singh, A., Prabhakar, P. K., Meghwal, M., & Upadhyay, A. (2022). Optimization and characterization of soybean oil-carnauba wax oleogel. *Lebensmittel-Wissenschaft & Technologie*, 157, Article 113108. <https://doi.org/10.1016/j.lwt.2022.113108>
- Wei, F., Miao, J., Tan, H., Feng, R., Zheng, Q., Cao, Y., & Lan, Y. (2021). Oleogel-structured emulsion for enhanced oxidative stability of perilla oil: Influence of crystal morphology and cooling temperature. *Lebensmittel-Wissenschaft & Technologie*, 139, Article 110560. <https://doi.org/10.1016/j.lwt.2020.110560>
- WHO. (2018). Healthy diet: Fact Sheet N°394. [https://www.who.int/nutrition/publications/nutrientrequirements/healthy\\_diet\\_fact\\_sheet\\_394.pdf?ua=1](https://www.who.int/nutrition/publications/nutrientrequirements/healthy_diet_fact_sheet_394.pdf?ua=1)
- Wijarnprecha, K., de Vries, A., Santiwattana, P., Sonwai, S., & Rousseau, D. (2019). Microstructure and rheology of oleogel-stabilized water-in-oil emulsions containing crystal-stabilized droplets as active fillers. *Lebensmittel-Wissenschaft & Technologie*, 115, Article 108058. <https://doi.org/10.1016/j.lwt.2019.04.059>
- Winkler-Moser, J. K., Anderson, J., Felker, F. C., & Hwang, H. S. (2019). Physical properties of beeswax, sunflower wax, and candellilla wax mixtures and oleogels [Article]. *Journal of the American Oil Chemists' Society*, 96(10), 1125–1142. <https://doi.org/10.1002/aocs.12280>
- Yang, S., Yang, G., Chen, X., Chen, J., & Liu, W. (2020). Interaction of monopalmitate and carnauba wax on the properties and crystallization behavior of soybean oleogel. *Grain & Oil Science and Technology*, 3(2), 49–56. <https://doi.org/10.1016/j.gaost.2020.05.001>
- Yang, S., Zhu, M., Wang, N., Cui, X., Xu, Q., Saleh, A. S. M., Duan, Y., & Xiao, Z. (2018). Influence of oil type on characteristics of  $\beta$ -sitosterol and stearic acid based oleogel. *Food Biophysics*, 13(4), 362–373. <https://doi.org/10.1007/s11483-018-9542-7>
- Yi, B., Kim, M.-J., Lee, S. Y., & Lee, J. (2017). Physicochemical properties and oxidative stability of oleogels made of carnauba wax with canola oil or beeswax with grapeseed oil. *Food Science and Biotechnology*, 26(1), 79–87. <https://doi.org/10.1007/s10068-017-0011-8>
- Yılmaz, E., & Demirci, Ş. (2021). Preparation and evaluation of virgin olive oil oleogels including thyme and cumin spices with sunflower wax. *Gels (Basel, Switzerland)*, 7(3). <https://doi.org/10.3390/gels7030095>
- Yılmaz, E., Keskin Uslu, E., & Öz, C. (2021). Oleogels of some plant waxes: Characterization and comparison with sunflower wax oleogel. *Journal of the American Oil Chemists' Society*, 98(6), 643–655. <https://doi.org/10.1002/aocs.12490>
- Yılmaz, E., & Ögütçü, M. (2014a). Comparative analysis of olive oil organogels containing beeswax and sunflower wax with breakfast margarine. *Journal of Food Science*, 79(9), E1732–E1738. <https://doi.org/10.1111/1750-3841.12561>
- Yılmaz, E., & Ögütçü, M. (2014b). Properties and stability of hazelnut oil organogels with beeswax and monoglyceride. *Journal of the American Oil Chemists' Society*, 91(6), 1007–1017. <https://doi.org/10.1007/s11746-014-2434-1>



Yılmaz, E., Uslu, E. K., & Toksöz, B. (2020). Structure, rheological and sensory properties of some animal wax based oleogels. *Journal of Oleo Science*, 69(10), 1317–1329. <https://doi.org/10.5650/jos.ess20081>

Zbikowska, A., Onacik-Gür, S., Kowalska, M., Sowiński, M., Szymańska, I., Żbikowska, K., Marciniak-Lukasiak, K., & Werpachowski, W. (2022). Analysis of

stability, rheological and structural properties of oleogels obtained from peanut oil structured with yellow beeswax. *Gels (Basel, Switzerland)*, 8(7). <https://doi.org/10.3390/gels8070448>

Zielonka, M., & Dobkowski, Z. (1998). Rheological characterization of damping materials based on polysiloxanes. In *Progress and trends in rheology V*. Heidelberg.